Available online at www.sciencedirect.com

SciVerse ScienceDirect

Geochimica et Cosmochimica Acta 106 (2013) 307–325

Geochimica et Cosmochimica Acta

www.elsevier.com/locate/gca

# Carbonate clumped isotope compositions of modern marine mollusk and brachiopod shells

Gregory A. Henkes [a,*], Benjamin H. Passey [a], Alan D. Wanamaker Jr. [b], Ethan L. Grossman [c], William G. Ambrose Jr. [d,e], Michael L. Carroll [e]

[a] Department of Earth & Planetary Sciences, The Johns Hopkins University, Baltimore, MD 21218, USA
[b] Department of Geological & Atmospheric Sciences, Iowa State University, Ames, IA 50011, USA
[c] Department of Geology & Geophysics, Texas A&M University, College Station, TX 77843, USA
[d] Department of Biology, Bates College, Lewiston, ME 04240, USA
[e] Akvaplan-Niva, Fram Center for Climate and Environment, N-9296 Tromsø, Norway

Received 1 June 2012; accepted in revised form 15 December 2012; Available online 3 January 2013

**Abstract**

We present an empirical calibration of the carbonate clumped isotope thermometer based on mollusk and brachiopod shells from natural and controlled environments spanning water temperatures of −1.0 to 29.5 °C. The clumped isotope data ($\Delta_{47}$) are normalized to $CO_2$ gases with equilibrium distributions of clumped isotopologues at high temperature (1000 °C) and low temperature (27 or 30 °C), and thus the calibration is unique in being directly referenced to a carbon dioxide equilibrium reference frame (Dennis et al., 2011, Defining an absolute reference frame for clumped isotope studies of $CO_2$, Geochimica et Cosmochimica Acta, **75**, 7117–7131). The shell clumped isotope data define the following relation as a function of temperature (in kelvin):

$$\Delta_{47} = 0.0327 \times 10^6/T^2 + 0.3286 \quad (r^2 = 0.84).$$

The temperature sensitivity (slope) of this relation is lower than those based on corals, fish otoliths, foraminifera, and coccoliths, but is similar to theoretical predictions for calcite based on lattice dynamics calculations. We find no convincing methodological or biological explanations for the difference in temperature sensitivity between this calibration and the previous calibrations, and suggest that the discrepancy might represent real but unknown differences in mineral–DIC clumped isotope fractionation between mollusks/brachiopods and other taxa. Nevertheless, revised analytical methods similar to those used in this study are now in wide use, and it will be important to develop calibrations for other taxonomic groups using these updated methods, with analyses directly referenced to the carbon dioxide equilibrium reference frame.


## 1. INTRODUCTION

Traditional oxygen isotope thermometry is based on the temperature dependence of isotope exchange between fluid and mineral. The carbonate-water oxygen isotope thermometer, which is commonly used to infer paleotemperature from ancient carbonates, requires knowledge of both the oxygen isotope composition ($\delta^{18}O$) of the mineral and the precipitating fluid (e.g., Epstein et al., 1953). The difficulty of constraining both temperature and the oxygen isotope composition of the coeval water from a single carbonate $\delta^{18}O$ measurement is a long-standing dilemma in oxygen isotope paleothermometry. Except for fluid inclusions and pore fluids (e.g., Schrag and DePaolo, 1993) there are few direct $\delta^{18}O$ measurements of natural waters beyond

* Corresponding author. Tel.: +1 410 516 7135; fax: +1 410 516 7933.
*E-mail address:* ghenkes1@jhu.edu (G.A. Henkes).

0016-7037/$ - see front matter © 2012 Elsevier Ltd. All rights reserved.
http://dx.doi.org/10.1016/j.gca.2012.12.020

the historical record, leaving the oxygen isotope paleothermometer underdetermined in most geologic applications. Reconstructing paleotemperature is the cornerstone of paleoclimatology and paleoceanography, but the absence of independent constraints on the isotopic composition of ancient waters has limited the application of the oxygen isotope paleothermometer. The 'clumped' isotope thermometer has emerged as an appealing alternative because, unlike carbonate $\delta^{18}O$ thermometry, it is independent of the bulk isotopic composition of water.

Clumped isotope thermometry examines the temperature dependence of bond formation between two rare, heavy isotopes within a single molecule (e.g., $^{13}C$ and $^{18}O$ forming the $^{13}C^{18}O$ isotopologue of carbon monoxide). This 'clumping' is based on homogeneous isotope exchange reactions which are independent of the bulk isotopic composition (e.g., $\delta^{13}C$, $\delta^{18}O$) of the phase. The relevant exchange reaction for carbonate clumped isotope thermometry is:

$$Ca^{13}C^{16}O_3 + Ca^{12}C^{18}O^{16}O_2 \leftrightarrow Ca^{13}C^{18}O^{16}O_2 + Ca^{12}C^{16}O_3.$$

This differs from traditional oxygen isotope thermometry, which is only concerned with 'singly-substituted isotopologues' of a molecule (e.g., $Ca^{12}C^{18}O^{16}O$). The carbonate clumped isotope thermometer is of particular interest because the temperature dependence of its enrichment has been predicted by theory (Schauble et al., 2006) and carbonate minerals are common in a range of natural environments. Precise measurement of multiple-substituted isotopologues in natural carbonates can therefore allow reconstructions of their formation temperatures. Additionally, clumped isotope-derived temperatures can be used in conjunction with the oxygen isotope thermometer to calculate the isotopic composition of the precipitating fluid. Because of these features, clumped isotope paleothermometry is becoming a widely used technique for reconstructing paleotemperature and the isotopic composition of ancient seawater (Came et al., 2007; Finnegan et al., 2011; Keating-Bitonti et al., 2011). Meaningful application of the carbonate clumped isotope paleothermometer, however, is contingent on the development of calibration curves that relate $\Delta_{47}$, a measure of $^{13}C$–$^{18}O$ clumping in carbonate, with known temperatures of mineralization. $\Delta_{47}$ is a function of the abundance of the mass-47 ($^{13}C^{18}O^{16}O$) isotopologue of $CO_2$ produced by acid digestion of a carbonate mineral and is calculated as:

$$\Delta_{47} = [(R^{47}/R^{47^*}) - (R^{46}/R^{46^*}) - (R^{45}/R^{45^*}) + 1] \times 1000 \quad (1)$$

where

$$R^i = \text{mass } i/\text{mass } 44 \quad (2)$$

is the ratio for the each isotopologue of $CO_2$ generated from carbonate, and the asterisk superscript indicates ratios with stochastic isotopologue abundances.

Experimental calibrations of the clumped isotope thermometer have been generated by measuring the $\Delta_{47}$ of calcium carbonate precipitated at temperatures from 1 to ~70 °C (Ghosh et al., 2006; Dennis and Schrag, 2010). Empirical calibrations have used biogenic carbonates produced by corals, foraminifera, coccolithophores, brachiopods, mollusks, and fishes from natural waters with known ambient growth temperatures (Ghosh et al., 2006, 2007; Came et al., 2007; Tripati et al., 2010; Thiagarajan et al., 2011). The majority of the calibration data have come from a laboratory at the California Institute of Technology (Caltech) and mostly conform to a single calibration line first described by Ghosh et al. (2006) (Fig. 1). Dennis and Schrag (2010), working at Harvard University and using slightly different analytical methods, developed an experimental (inorganic) calcite $\Delta_{47}$–temperature calibration which deviated substantially from the Ghosh et al. (2006) calibration line at temperatures below ~20 °C. The Dennis and Schrag (2010) data, however, closely align with theoretical predictions of the temperature sensitivity of the carbonate clumped isotope thermometer for calcite minerals by Schauble et al. (2006) and Guo et al. (2009) (Fig. 1).

Unresolved differences between empirical calibrations have been a driving force behind interlaboratory comparisons designed to evaluate consistency between laboratories generating clumped isotope data (e.g., Dennis et al., 2011), as well as continued analysis of natural carbonates with well-constrained growth temperatures, such as modern land snails (Zaarur et al., 2011). Marine mollusks and brachiopods have so far escaped detailed calibration, although Came et al. (2007) report a limited dataset that conforms to the Caltech calibration line. A more comprehensive

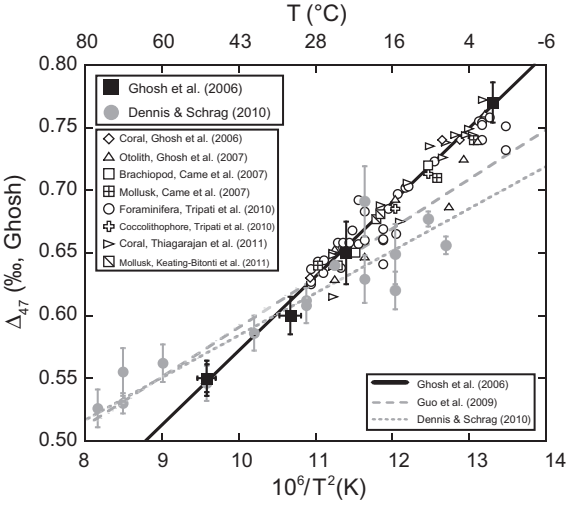


Fig. 1. Carbonate clumped isotope values ($\Delta_{47}$) from existing temperature (T) calibrations. The solid symbols are data from inorganic calcite precipitation experiments (Ghosh et al., 2006; Dennis and Schrag, 2010) and the solid black and dotted gray lines are linear regressions through each dataset, respectively. The dashed gray curve is the theoretical $\Delta_{47}$–temperature relationship for calcite from Guo et al. (2009). Open symbols are data from natural and cultured biogenic carbonates. Error bars on $\Delta_{47}$ represent the standard error from multiple analyses of a single sample, and error bars are not shown for the biogenic data to improve clarity. Clumped isotope data are reported on the heated gas or 'Ghosh' reference frame described by Ghosh et al. (2006) and Huntington et al. (2009). Error bars on $10^6/T^2$ represent the reported error for carbonate precipitation temperatures.

clumped isotope calibration, which spans a wider range of growth temperatures and a diversity of taxa, remains to be developed for these groups.

Additionally, few laboratories continue to utilize the analytical methods used to generate the Caltech calibrations reported in Ghosh et al. (2006, 2007), Came et al. (2007), Tripati et al. (2010), and Thiagarajan et al. (2011). These methods include 25 °C acid reactions in sealed vessels, use of a capillary gas chromatography (GC) column for purification of $CO_2$, and normalization of data to a single equilibrium $CO_2$ gas composition (1000 °C 'heated gases'; see Huntington et al., 2009). Most laboratories, including Caltech, now use online extraction systems where carbonates are reacted in hot acid (typically 70–90 °C), $CO_2$ is continuously removed during the reaction by collection onto a cryogenic trap, and the $CO_2$ is purified by passage through traps or packed GC columns filled with a divinylbenzene polymer (Porapak Q™). In addition, an improved reference frame has recently been proposed (Dennis et al., 2011) whereby data are normalized to equilibrium $CO_2$ prepared at at least two temperatures, typically one high temperature (1000 °C) and one low temperature (~25 °C). As such, there is now additional motivation to generate new calibrations, using the newer analytical methods, and within the framework of concurrent analyses of $CO_2$ gas in isotopologue equilibrium at two or more widely spaced temperatures.

In this paper we describe the results of a calibration of the carbonate clumped isotope thermometer for modern marine mollusks and brachiopods. The samples were obtained from natural marine environments or grown under monitored conditions in waters spanning a range of temperatures (−1.0 to 29.5 °C). Both of the major mineralogies of brachiopods and mollusks, calcite and aragonite, were examined. The $\Delta_{47}$ data are the first calibration data to be reported on a new reference frame for multiple isotopologue analyses of $CO_2$. Our study also employs laboratory methods similar to those now in wide usage.

## 2. MATERIALS AND METHODS

### 2.1. Samples

The calibration was generated using shell material from 16 different mollusk and brachiopod species, spanning a range of growth environments and shell morphologies (Table 1). The majority of the organisms were collected live from the benthos, including shallow coastal areas, on the continental shelf, or in the deep-sea. Mollusks were collected from the northwestern Barents Sea (Spitsbergen Bank, Norway; Carroll et al., 2011), the northern Icelandic shelf (Grimsey Island, Iceland; Wanamaker et al., 2008), the northern Gulf of Mexico (Stetson Bank, USA; Gentry et al., 2008), and the coastal waters of southwest Puerto Rico. Other shells were grown in controlled conditions that were monitored for changes in temperature and the oxygen isotopic composition of water. The temperate bivalve mollusks *Mytilus edulis* and *Mya arenaria* were grown in tanks at the Darling Marine Center (University of Maine, Walpole, ME, USA), located on the Gulf of Maine coast, using tidally-influenced water from the Damariscotta River (Wanamaker et al., 2007). Oysters, *Crassostrea virginica*, were grown in aquaculture cages at the Horn Point Marine Laboratory (University of Maryland, Cambridge, MD, USA) and nautiloids, *Nautilus pompilius*, were obtained from the Toba Aquarium (Toba, Japan). The brachiopods used in this study are from Antarctica (South Shetland Islands), the northern Gulf of Mexico, coastal California (Half Moon Bay, CA, USA), and the northern Caribbean Sea (Rio Bueno Harbor, Jamaica). Water temperatures at the collection locations ranged from 20 to 31 °C in the subtropics and tropics, to less than <0 °C in high-latitude seas.

The mineralogy of some mollusk shells was confirmed by powder X-ray diffraction using a Philips X'Pert Pro MPD diffractometer in the Department of Materials Science and Engineering at Johns Hopkins University, Baltimore, MD (Electronic Annex, Fig. 1). The shells of *N. pompilius* (Japan), *Hiatella arctica*, *Mya truncata*, *Astarte crenata*, *Astarte borealis*, *Clinocardium ciliatum* (all from the Barents Sea), *Phacoides pectinata* (Puerto Rico), and *M. arenaria* (Maine, USA) are all aragonite, whereas the shells of *Chlamys islandica* (Barents Sea) are calcite. *M. edulis* (Maine, USA) shells contain both calcite and aragonite, but only the calcitic component of these shells was sub-sampled for clumped isotope analysis (Wanamaker et al., 2007).

#### 2.1.1. Mollusk growth temperatures

Generating this calibration required knowledge of the ambient shell growth temperatures of both natural and controlled environments. For shells collected in regions where long-term temperature records did not exist we relied on nearby records or direct temperature readings made during collections. In the northwestern Barents Sea mollusks were collected at two sites in an area where Arctic and Atlantic water masses, each of different temperature, converge (see Carroll et al., 2011 for detailed collection information). The collection sites were located on either side of the Polar Front, an oceanographic boundary between the water masses. The position of the Polar Front may vary by kilometers annually, but is tightly constrained in the collection area by steep seafloor topography and regional circulation (Johannessen and Foster, 1978; Harris et al., 1998). Bottom temperatures in Arctic waters north of the Polar Front at site 'B-12' were $-1 \pm 2$ °C at a depth of 99 m, whereas bottom temperatures in the warmer Atlantic water south of the Polar Front at site 'B-14' were $2 \pm 2$ °C at 187 m (Harris et al., 1998; Carroll et al., 2011). In summer 2007, live, undamaged bivalves were collected at each site, immediately shucked, and frozen aboard the R/V Lance (Norwegian Polar Institute, Tromsø, Norway). Using sclerochronological analyses of these same shells Carroll et al. (2011) demonstrated that *C. ciliatum* specimens collected at both sites were ⩾25 years old. Because shell analyzed from all Arctic species represented a 'bulk' sample, which integrated across the entire shell, it is possible that decadal-scale variations in seawater temperature caused additional error in our growth temperature assignments for these sites. The longest instrumental temperature record from the Barents Sea along the Kola Transect shows that decadal variability in sea surface temperature (<200 m)

Table 1
Carbon ($\delta^{13}C$), oxygen ($\delta^{18}O$), and clumped ($\Delta_{47}$) isotope compositions of marine mollusks and brachiopods.

| Sample ID | Depth (m) | Growth Temp. (°C) | Temp. Range (±°C) | Salinity (‰) | Class[a] | Species | *n* | $\delta^{13}C_{carb}$ (‰, PDB) | $\delta^{18}O_{carb}$ (‰, PDB) | $\delta^{18}O_{water}$ (‰, SMOW)[b] | $\Delta_{47}$ (‰, Ghosh)[c] | $\Delta_{47}$ (‰, CDES)[d] |
|---|---|---|---|---|---|---|---|---|---|---|---|---|
| Mollusks | | | | | | | | | | | | |
| *B-12, northwestern Barents Sea (Polar water), 75°39.80′N, 24°01.14′E* | | | | | | | | | | | | |
| Ha-1 | 99 | −1.0 | 2.0 | 34.5 | Bivalvia (ar) | *Hiatella arctica* | 3 | 1.29 (±0.02) | 5.08 (±0.02) | *0.72* | 0.708 | 0.768 (±0.004) |
| Ha-2 | 99 | −1.0 | 2.0 | 34.5 | Bivalvia (ar) | *Hiatella arctica* | 3 | 1.42 (±0.06) | 4.92 (±0.09) | *0.72* | 0.726 | 0.783 (±0.006) |
| Ha-3 | 99 | −1.0 | 2.0 | 34.5 | Bivalvia (ar) | *Hiatella arctica* | 3 | 0.41 (±0.03) | 5.05 (±0.04) | *0.72* | 0.719 | 0.776 (±0.005) |
| Mt-1 | 99 | −1.0 | 2.0 | 34.5 | Bivalvia (ar) | *Mya truncata* | 3 | 1.71 (±0.01) | 5.38 (±0.01) | *0.72* | 0.707 | 0.772 (±0.006) |
| Mt-2 | 99 | −1.0 | 2.0 | 34.5 | Bivalvia (ar) | *Mya truncata* | 4 | 1.98 (±0.01) | 5.49 (±0.03) | *0.72* | 0.693 | 0.757 (±0.010) |
| Mt-3 | 99 | −1.0 | 2.0 | 34.5 | Bivalvia (ar) | *Mya truncata* | 3 | 2.07 (±0.01) | 5.52 (±0.01) | *0.72* | 0.709 | 0.775 (±0.007) |
| Ci-1 | 99 | −1.0 | 2.0 | 34.5 | Bivalvia (c) | *Chlamys islandica* | 3 | 1.22 (±0.01) | 4.43 (±0.02) | *0.72* | 0.713 | 0.782 (±0.009) |
| Ci-2 | 99 | −1.0 | 2.0 | 34.5 | Bivalvia (c) | *Chlamys islandica* | 3 | 1.02 (±0.01) | 4.45 (±0.01) | *0.72* | 0.697 | 0.763 (±0.005) |
| Ci-3 | 99 | −1.0 | 2.0 | 34.5 | Bivalvia (c) | *Chlamys islandica* | 5 | 1.02 (±0.01) | 4.56 (±0.02) | *0.72* | 0.717 | 0.784 (±0.007) |
| Ac-1 | 99 | −1.0 | 2.0 | 34.5 | Bivalvia (ar) | *Astarte crenata* | 3 | 1.50 (±0.04) | 5.29 (±0.01) | *0.72* | 0.711 | 0.781 (±0.003) |
| Ab-1 | 99 | −1.0 | 2.0 | 34.5 | Bivalvia (ar) | *Astarte borealis* | 3 | 0.76 (±0.01) | 5.35 (±0.02) | *0.72* | 0.694 | 0.764 (±0.011) |
| Ab-2 | 99 | −1.0 | 2.0 | 34.5 | Bivalvia (ar) | *Astarte borealis* | 3 | 1.03 (±0.02) | 5.37 (±0.01) | *0.72* | 0.707 | 0.773 (±0.004) |
| Ab-3 | 99 | −1.0 | 2.0 | 34.5 | Bivalvia (ar) | *Astarte borealis* | 3 | 0.73 (±0.03) | 5.27 (±0.01) | *0.72* | 0.692 | 0.758 (±0.017) |
| Cc-1 | 99 | −1.0 | 2.0 | 34.5 | Bivalvia (ar) | *Clinocardium ciliatum* | 3 | 0.27 (±0.01) | 4.40 (±0.01) | *0.72* | 0.686 | 0.753 (±0.007) |
| Cc-2 | 99 | −1.0 | 2.0 | 34.5 | Bivalvia (ar) | *Clinocardium ciliatum* | 3 | −0.96 (±0.02) | 4.26 (±0.03) | *0.72* | 0.682 | 0.745[e] |
| *B-14, northwestern Barents Sea (Atlantic water), 75°00.06′N, 24°05.82′E* | | | | | | | | | | | | |
| Ac-1 | 187 | 2.0 | 2.0 | 34.8 | Bivalvia (ar) | *Astarte crenata* | 3 | 1.14 (±0.01) | 4.88 (±0.01) | *0.66* | 0.717 | 0.788 (±0.004)[f] |
| Ac-2 | 187 | 2.0 | 2.0 | 34.8 | Bivalvia (ar) | *Astarte crenata* | 3 | 1.08 (±0.03) | 4.89 (±0.02) | *0.66* | 0.693 | 0.759 (±0.007) |
| Cc-1 | 187 | 2.0 | 2.0 | 34.8 | Bivalvia (ar) | *Clinocardium ciliatum* | 3 | −0.20 (±0.04) | 4.19 (±0.01) | *0.66* | 0.690 | 0.756 (±0.013) |
| Cc-2 | 187 | 2.0 | 2.0 | 34.8 | Bivalvia (ar) | *Clinocardium ciliatum* | 3 | −0.38 (±0.10) | 4.12 (±0.02) | *0.66* | 0.689 | 0.758 (±0.011) |
| Cc-3 | 187 | 2.0 | 2.0 | 34.8 | Bivalvia (ar) | *Clinocardium ciliatum* | 3 | −0.40 (±0.03) | 4.19 (±0.03) | *0.66* | 0.698 | 0.765 (±0.006) |
| *Grimsey Island, Icelandic Sea, 66°31.59′N, 18°11.74′W* | | | | | | | | | | | | |
| WG061278 | 83 | 4.7 | 2.0 | 34.9 | Bivalvia (ar) | *Arctica islandica* | 3 | 1.40 (±0.02) | 3.62 (±0.02) | 0.08 | 0.660 | 0.729 (±0.008) |
| *Stetson Bank, Gulf of Mexico, USA, 28°09.96′N, 94°17.82′W* | | | | | | | | | | | | |
| FGS-1-1 | 24 | 27.5 | 2.2 | ⩾34.0 | Gastropoda (ar) | *Conus ermineus* | 3 | −0.30 (±0.01) | −0.84 (±0.06) | 1.34 | 0.593 | 0.656 (±0.007) |
| FGS-1-2 | 24 | 23.0 | 1.5 | ⩾34.0 | Gastropoda (ar) | *Conus ermineus* | 3 | −0.04 (±0.01) | −0.22 (±0.02) | 0.99 | 0.625 | 0.692 (±0.005) |
| FGS-1-3 | 24 | 19.8 | 0.8 | ⩾34.0 | Gastropoda (ar) | *Conus ermineus* | 3 | −0.14 (±0.01) | 0.60 (±0.01) | 0.68 | 0.630 | 0.697 (±0.007) |
| *La Parguera, Puerto Rico, USA, 17°95.00′N, 67°04.83′W* | | | | | | | | | | | | |
| Pp-1 | 1 | 29.5 | 3.0 | ⩾35.0 | Bivalvia (ar) | *Phacoides pectinatus* | 3 | 0.90 (±0.07) | −0.55 (±0.07) | *0.80* | 0.624 | 0.690 (±0.003) |
| Pp-2 | 1 | 29.5 | 3.0 | ⩾35.0 | Bivalvia (ar) | *Phacoides pectinatus* | 3 | 0.77 (±0.01) | −0.70 (±0.02) | *0.80* | 0.632 | 0.699 (±0.013) |
| Pp-3 | 1 | 29.5 | 3.0 | ⩾35.0 | Bivalvia (ar) | *Phacoides pectinatus* | 3 | 1.07 (±0.02) | −0.72 (±0.04) | *0.80* | 0.629 | 0.693 (±0.008) |
| *University of Maine Darling Marine Center, Damariscotta River, Maine, USA, 43°51.75′ N, 69°34.88′ W* | | | | | | | | | | | | |
| Mya-3.5 | – | 3.4 | 0.8 | 30.4 | Bivalvia (ar) | *Mya arenaria* | 2 | 1.42 (±0.01) | 0.41 (±0.02) | −1.57 | 0.670 | 0.740 (±0.020) |
| Mya-8.5 | – | 8.6 | 2.2 | 29.9 | Bivalvia (ar) | *Mya arenaria* | 3 | 1.34 (±0.01) | −0.45 (±0.04) | −1.66 | 0.649 | 0.718 (±0.007) |
| Mya-16 | – | 15.9 | 1.7 | 30.7 | Bivalvia (ar) | *Mya arenaria* | 3 | 0.95 (±0.01) | −0.82 (±0.04) | −1.38 | 0.646 | 0.715 (±0.003) |
| Mytilus-4 | – | 4.0 | 0.5 | 32.0 | Bivalvia (c) | *Mytilus edulis* | 5 | −6.47 (±0.03) | 0.67 (±0.04) | −1.94 | 0.699 | 0.776 (±0.007)[g] |
| Mytilus-8 | – | 8.0 | 0.5 | 32.0 | Bivalvia (c) | *Mytilus edulis* | 4 | −7.89 (±0.02) | −1.40 (±0.03) | −3.07 | 0.680 | 0.757 (±0.009)[g] |

| | | | | | | | | | | | | |
|---|---|---|---|---|---|---|---|---|---|---|---|---|
| Mytilus-12 | – | 12.0 | 0.5 | 32.0 | Bivalvia (c) | *Mytilus edulis* | 2 | −6.25 (±0.02) | −1.11 (±0.02) | −2.03 | 0.691 | 0.769 (±0.017)[g] |
| Mytilus-15 | – | 15.0 | 0.5 | 32.0 | Bivalvia (c) | *Mytilus edulis* | 4 | −6.82 (±0.01) | −1.34 (±0.04) | −1.37 | 0.665 | 0.741 (±0.005)[g] |
| *University of Maryland Horn Point Laboratory, Choptank River, Maryland, USA, 38°35.60′N, 76°07.74′W* | | | | | | | | | | | | |
| HPL-1 | – | 14.4 | 0.5 | 13.5 | Bivalvia (c) | *Crassostrea virginica* | 3 | −4.23 (±0.05) | −1.96 (±0.03) | −3.76 | 0.664 | 0.735 (±0.004) |
| HPL-2 | – | 27.3 | 0.2 | 11.6 | Bivalvia (c) | *Crassostrea virginica* | 2 | −5.30 (±0.02) | −6.01 (±0.02) | −3.54 | 0.616 | 0.686 (±0.005) |
| HPL-3 | – | 23.7 | 0.1 | 13.2 | Bivalvia (c) | *Crassostrea virginica* | 3 | −5.24 (±0.03) | −3.99 (±0.01) | −3.69 | 0.640 | 0.708 (±0.007) |
| *Toba Aquarium, Toba, Japan, 34°29.00′N, 136°51.00′E* | | | | | | | | | | | | |
| P8/30 | – | 24.5 | 0.5 | – | Cephalopoda (ar) | *Nautilus pompilius* | 3 | −0.43 (±0.02) | −1.10 (±0.05) | *−0.34* | 0.661 | 0.726 (±0.005) |
| P52 | – | 24.5 | 0.5 | – | Cephalopoda (ar) | *Nautilus pompilius* | 3 | −2.55 (±0.09) | −0.89 (±0.13) | *−0.34* | 0.652 | 0.717 (±0.003) |
| P132 | – | 24.5 | 0.5 | – | Cephalopoda (ar) | *Nautilus pompilius* | 3 | −3.63 (±0.03) | −0.71 (±0.04) | *−0.34* | 0.661 | 0.726 (±0.008) |
| P110 | – | 20 | 1.0 | – | Cephalopoda (ar) | *Nautilus pompilius* | 3 | −4.06 (±0.03) | −0.33 (±0.03) | *−0.34* | 0.633 | 0.696 (±0.012) |
| P95 | – | 20 | 1.0 | – | Cephalopoda (ar) | *Nautilus pompilius* | 3 | −3.82 (±0.01) | −0.06 (±0.01) | *−0.34* | 0.634 | 0.706 (±0.009) |
| P105 | – | 20 | 1.0 | – | Cephalopoda (ar) | *Nautilus pompilius* | 3 | −3.21 (±0.01) | −0.20 (±0.03) | *−0.34* | 0.637 | 0.709 (±0.004) |
| Brachiopods | | | | | | | | | | | | |
| *Admiralty Bay, South Shetland Islands (Southern Ocean), 62°10.00′N, 58°25.00′W* | | | | | | | | | | | | |
| GB4–3 | 250–300 | −1.0 | 1.0 | 34.5 | Rhychonellata (c) | *Magellania* spp. | 3 | 0.54 (±0.04) | 3.50 (±0.03) | *−0.20* | 0.709 | 0.785 (±0.007) |
| GB3–5 | 250–300 | −1.0 | 1.0 | 34.5 | Rhychonellata (c) | *Magellania* spp. | 3 | 0.99 (±0.01) | 3.48 (±0.02) | *−0.20* | 0.693 | 0.773 (±0.013) |
| *North Central Gulf of Mexico, USA, 27°09.96′N, 94°17.82′W* | | | | | | | | | | | | |
| Brach-m1 | 742 | 5.5 | – | – | Rhychonellata (c) | *Ecnomiosa gerda* | 3 | 1.48 (±0.02) | 3.02 (±0.04) | *0.00* | 0.690 | 0.756 (±0.005) |
| Brach-m2 | 742 | 5.5 | – | – | Rhychonellata (c) | *Ecnomiosa gerda* | 3 | 1.56 (±0.02) | 3.10 (±0.09) | *0.00* | 0.691 | 0.757 (±0.014) |
| *Half Moon Bay, CA, USA, 37°27.32′N, 122°26.13′W* | | | | | | | | | | | | |
| HMB-3 | 55 | 10.5 | 1 | 33.2 | Rhychonellata (c) | *Terebratulina unguicula* | 2 | 1.09 (±0.01) | 1.22 (±0.01) | *0.10* | 0.681 | 0.754 (±0.002) |
| *Rio Bueno Harbor, Jamaica 18°28.12′N, 77°27.50′W* | | | | | | | | | | | | |
| RBJ-1-3 | 20 | 27.5 | – | 35.9 | Rhychonellata (c) | *Lacazella* spp. | 3 | 2.07 (±0.04) | −1.00 (±0.07) | *0.80* | 0.614 | 0.676 (±0.011) |

*Note:* All ± values are standard error of the mean ($=1\sigma/\sqrt{n}$), where $1\sigma$ is the standard deviation of the n analyses (each analysis consists of extraction of $CO_2$ from carbonate, purification of the $CO_2$, and analysis in the mass spectrometer over six 'acquisitions', as detailed in Section 2.2.).

[a] (ar) = aragonite shell, (c) = calcite shell. In some cases this was confirmed by X-ray powder diffraction (Fig. 1, Electronic Annex).

[b] Water oxygen isotope values were either measured directly or taken from the model of LeGrande and Schmidt (2006) using the sample coordinates and collection depths (model values are in *italics*).

[c] Values reported on the heated gas or 'Ghosh' scale described by Ghosh et al. (2006) and Huntington et al. (2009).

[d] Values reported on the carbon dioxide equilibrium scale or 'CDES' described by Dennis et al. (2011).

[e] Duplicate and triplicate values were rejected because of high $\Delta_{48}$ values; possibly contaminated (Table 1, Electronic Annex).

[f] High $\Delta_{47}$ value compared to other shells analyzed from this location. No methodological reason to reject data.

[g] Divergent $\Delta_{47}$ values for carbonate standards run with these samples. The values of NBS-19 were greater than its working value (0.352‰) for JHU Sequence Numbers 382 and 409. Samples were rejected on these grounds.

did not exceeded ±1 °C from ~1900 to 2000 (Skagseth et al., 2008). This implies that measured sub-annual temperature variability of ±2 °C is greater than the annual and decadal variability over the last 100 years of shell growth in the Barents Sea.

One shell of the mollusk *Arctica islandica* was included in our calibration. This specimen was collected live from the northern Icelandic Shelf southwest of the island of Grimsey, Iceland at a depth of 83 m in June 2006 (Wanamaker et al., 2008). Based on counts of annual growth bands this organism lived from 1981 to 2006. Bottom temperatures on the northern Icelandic Shelf over this interval were estimated to be 4.7 ± 2 °C by averaging summer (JJA) measurements from 50 and 100 m depth along the Siglunes 3 profile, which is located ~25 km west of the collection location (data from the Marine Research Institute, Reykjavik, Iceland; see Knudsen et al., 2004). The average annual temperature range (1947–2006) is ~1.8 °C at Siglunes 3, which is greater than variability in the average monthly temperature (JJA, ±0.9 °C). Because the *A. islandica* shell was sub-sampled across all growth years, we used ±2 °C as a conservative estimate of the assigned temperature error.

A single specimen of the gastropod *Conus ermineus* was obtained for this study (see Gentry et al., 2008). This organism was collected live from the Stetson Bank in the northern Gulf of Mexico in 2003 at 24 m water depth, but died shortly after collection. Bottom growth temperatures were monitored from November 2002 to January 2004 using data loggers deployed at the collection site by Post, Buckley, Schuh & Jernigan, Inc. (PBS & J Inc.) under contract to the Flower Garden Banks National Marine Sanctuary. From 2002 to 2004, the bottom temperatures on the Stetson Bank ranged from 17 to 30 °C, with a mean temperature of 22.6 °C (Gentry et al., 2008). This relatively large seasonal temperature range precluded the use of 'bulk' shell from *C. ermineus* in our calibration. Instead, we sampled intra-annual shell material from within a single growth year. By sub-sampling within 1 year we effectively decreased the temperature range associated with a single isotopic measurement. To do this we identified the most recent external growth band and sub-sampled from three divisions corresponding to the 2002 growth year using a Dremel© rotary drill. The sub-sampled areas were determined by scaling the sub-sampling intervals in Gentry et al. (2008) to another part of the shell. This sampling method allowed for direct comparison with the temperatures and seawater oxygen isotope measurements reported by Gentry et al. (2008).

Three shells of the bivalve mollusk *P. pectinatus* were collected in January 2010 from a mangrove lagoon located near the town of La Parguera, Puerto Rico. The bivalves were found buried in organic-rich sediment in 1 m of water. The 'Pithahaya' lagoon is subtidal and, because there are no significant local sources of freshwater, is fully marine with salinities in excess of 35‰ (Rooker and Dennis, 1991). Monthly sea surface temperatures (SST) recorded at a nearby coral reef over a 30 year period from 1966 to 1995 ranged from 25 to 30 °C with a mean of ~29.5 °C (Winter et al., 1998). Over 30 years the mean SST increased by 0.7 °C, which was significant but still smaller than the seasonal temperature range of 3 °C used as our estimate of growth temperature variability. *P. pectinatus* shell material used for clumped isotope analysis was sampled across all growth bands.

Shells from two species of temperate marine bivalves were used in this calibration. These organisms were grown under controlled and continuously monitored environmental conditions at the University of Maine, Darling Marine Center in Walpole, ME, USA. Because seasonal temperature gradients in the Gulf of Maine can be large (16 °C) it was necessary to use 'cultured' shell grown at several constant, intermediate temperatures (~5 to 15 °C). We used shell material from the ventral margin of blue mussels, *M. edulis*, grown over intervals of 5–6 months at four temperatures (4, 8, 12, and 15 °C; reported in Wanamaker et al., 2007). Over these time periods only ~3 mm of new shell was grown. Because at least 30 mg of shell carbonate was required for replicate clumped isotope analyses (3 × 10 mg/analysis) we combined several individual shells from identical experimental conditions to obtain enough material for analysis. Water samples were collected weekly to monitor ambient changes in the seawater oxygen isotope value (Wanamaker et al., 2007). The soft shell clams, *M. arenaria*, used were also grown at the Darling Marine Center but the growth environments of these shells were not controlled. Instead, they lived in tanks fed with ambient water from the Damariscotta River. Shell growth was monitored from January to August 2010, over which time the water temperature warmed from ~2 to 18 °C. Calcein, a fluorescent dye which is commonly used for labeling shell, was used to mark three intervals in the shells which were later sub-sampled (see Beirne et al., 2012). This divided the 16 °C range in growth temperature into three periods: winter (average temp. = 3.39 ± 0.83 °C), spring (average temp. = 8.64 ± 2.18 °C), and summer (average temp. = 15.87 ± 1.65 °C).

Estuarine bivalves have traditionally been avoided in oxygen isotope thermometry because the temperature and oxygen isotope fluctuations (from meteoric water–seawater mixing) in mesohaline waters are covariable and therefore difficult to independently constrain. Because clumped isotope thermometry is independent of the isotopic composition of the ambient fluid we included eastern oysters, *C. virginica*, from the Choptank River in the Chesapeake Bay in this calibration. These specimens were grown in natural waters at the University of Maryland, Horn Point Laboratory in Cambridge, MD, USA. Oyster growth temperatures were monitored from August to November 2010, and shell was sampled from three intervals within this period corresponding to August (average temp. = 27.3 ± 0.2 °C), August–September (average temp. = 23.7 ± 0.4 °C), and September–November (average temp. = 14.4 ± 0.5 °C). The oxygen isotope composition of the waters was also monitored periodically.

Lastly, several nautilus shells (*N. pompilius*) were obtained from the Toba Aquarium in Toba, Japan. Adult *Nautili* were maintained in recirculating aquaria which used natural seawater held at a constant temperature of 20 ± 1 °C. The Toba nautiluses are one of the only broods in the world that successfully reproduce in captivity (T.

Moritaki, personal communication). Deposited eggs are transferred to warmer recycled seawater held at $25 \pm 0.5$ °C in a smaller 'incubation tank' where they are allowed to hatch and grow for 1–2 months. We analyzed 'bulk' shell material from both juvenile and adult shells.

*2.1.2. Brachiopod growth temperatures*

The articulate brachiopods used in this study were all collected live from their natural habitats (Table 1). Two specimens identified as *Magellania* spp. were obtained from Admirality Bay in the South Shetland Islands, Antarctica. Here the collection depth was 250–300 m with a mean annual temperature of $-1 \pm 1$ °C. Two specimens of the species *Ecnomiosa gerda* were collected in 742 m of water at 5.5 °C in the north-central Gulf of Mexico on the continental slope off of Texas, USA near site 83G3-6 in Grossman and Ku (1986). One specimen of *Terebratulina unguicula* was collected at 55 m depth in Half Moon Bay off the coast of California where waters were $10.5 \pm 1.0$ °C, and one specimen identified as *Lacazella* spp. was collected from Rio Bueno Harbor, Jamaica in 20 m of water which was ~27.5 °C (NODC World Ocean Atlas, http://www.esrl.noaa.gov/psd/data/gridded/data.nodc.woa98.html; Jackson and Winston, 1982). Brachiopod shell material came from the whole pedicle valve or was sub-sampled from one valve, perpendicular to the growth axis, across all growth bands.

### 2.2. Stable isotope measurements

Isotopic measurements were performed at John Hopkins University in the Department of Earth and Planetary Science using a Thermo Scientific MAT 253 mass spectrometer coupled to a custom-built, automated acid reaction and gas purification line. This line is nearly identical to the one described by Passey et al. (2010), and contains three coupled systems designed to generate high-purity $CO_2$ gas from carbonate samples and standards, and reference 'equilibrium $CO_2$ gases'. In the first stage, ~10 mg of carbonate is reacted *in vacuo* for 10 min in a common acid bath containing phosphoric acid ($\rho = 1.91$ mg/ml) held at 90 °C. The $CO_2$ gas is collected in a liquid nitrogen (LN) trap after passing through a −78 °C water trap. In the second stage the sample $CO_2$ is transferred from the collection trap (warmed to −78 °C) to a second LN trap using a purified He carrier gas. During this transfer the sample and carrier gas pass through a second −78 °C trap, a getter containing silver wool (to remove sulfur-containing contaminants), and finally a 1.2 m gas chromatography (GC) column containing Porapak™ porous polymer absorbent held at −20 °C. Prior to August 2011 the system did not use a silver wool getter. The addition of the getter had no obvious impact on the isotopic compositions of samples or standards. The last stage consists of a final transfer from the post-GC LN collection trap (warmed to −78 °C) to a smaller LN trap. This is done *in vacuo* after the He carrier gas is pumped away. The frozen sample $CO_2$ is then allowed to expand at room temperature for 3 min in the final trap before further expansion into the bellows of the MAT 253 dual inlet system. The other bellows contained a reference gas (Oztech Trading Corporation, Safford, AZ, USA) with a bulk isotopic composition of $\delta^{13}C = -3.61‰$ PDB and $\delta^{18}O = -15.81‰$ PDB.

Accurate carbonate clumped isotope measurements require a reference frame which corrects for changes in the ionization conditions inside of a gas source mass spectrometer and for 'nonlinearities' such as a dependence of the apparent $\Delta_{47}$ value on $\delta_{47}$ (where the latter is a measure of the $^{13}C$ and $^{18}O$ content of the sample; see Huntington et al., 2009; Dennis et al., 2011). This also allows all laboratories measuring clumped isotopes to report their data on a common scale (Dennis et al., 2011). To construct this reference frame, we regularly analyzed $CO_2$ gases driven to isotopologue equilibrium at 1000 °C and 30 or 27 °C. The former were prepared by heating aliquots of $CO_2$ in quartz tubes in a tube furnace held at 1000 °C. The latter were prepared by equilibrating $CO_2$ with water at a temperature of 30 or 27 °C (Fig. 2). Prior to May 2010 the equilibrations were done at 27 °C; subsequently all equilibrations were done at 30 °C. For each of these temperatures, we used two different $CO_2$ (or $H_2O$) reservoirs of differing bulk composition, so that in total four different equilibrium gases were analyzed. We analyzed one of these gases every 1–2 days, thus cycling through the four gases on a weekly or sub-weekly basis. These gases were introduced into a He carrier gas 'upstream' of the second stage of the purification line, and thus were treated in exactly the same manner as carbonates except for the initial acid extraction step.

Each sample, standard, or reference gas was analyzed at a bellows pressure corresponding to a signal of 12 V on the Faraday cup measuring mass 44 $CO_2$. The measurement sequence consisted of six repetitions of nine cycles, each with 26 s of integration time for a total combined integration of 1404 s per gas. The long-term internal standard deviation for $\Delta_{47}$ on the six repetitions of nine cycles was approximately 0.030‰. Most of the mollusk and brachiopod shells were run in triplicate, in which case the combined integration time approached the asymptotic portion of the shot noise curve predicted for carbonate clumped isotope analyses (Thiagarajan et al., 2011). The reported isotope ratios were calculated from these measurements. In some cases replicate measurements for a single sample (e.g., Ha-2) were all made during a single analytical session. It is possible that the reported error for these samples is artificially small because all analyses were corrected using the same reference frame. However, most samples used for this calibration were analyzed (replicated) over several analytical sessions.

### 2.3. Data reduction and analysis

Post-analysis data reduction was done according to the scheme outlined by Dennis et al. (2011) in which the equilibrium $CO_2$ gases are used to construct an empirical transfer function (ETF) that maps the measured sample $\Delta_{47}$ values onto a reference frame anchored to theoretical predictions of $\Delta_{47}$ of $CO_2$ gas at two different equilibration temperatures: 27 or 30 °C, and 1000 °C. It has been observed that the raw $\Delta_{47}$ values of the equilibrium $CO_2$ gases may drift over time due to changes in the physical state of mass spectrometers (Huntington et al., 2009; Passey et al.,

2010), causing the slope and intercept of the ETF to drift. To correct for this drift we used a MATLAB® script that models changes in the slope and intercept of the equilibrium gas lines as low-order polynomial functions of time using a least squares approximation (Passey et al., 2010). Occasionally, there was no discernible drift in the reference gas lines. When this was the case a static correction was used, where the equilibrium gas data were simply linearly regressed, not modeled. The ETF scheme also differs from previous attempts to establish a $\Delta_{47}$ reference frame (e.g., the heated gas line) because it does not depend on assumptions about (or calibration of) the $\Delta_{47}$ value of the dual inlet reference gas $CO_2$ (Ghosh et al., 2006; Huntington et al., 2009; Dennis et al., 2011). An acid temperature correction factor was applied to all data to normalize values to acid extractions performed at 25 °C. For the values reported on the original 'Ghosh' scale, we used an acid correction factor of 0.081‰ (Passey et al., 2010). For values reported on the new 'carbon dioxide equilibrium scale', we used a value of 0.092‰, a value that was determined by analyzing three different shells using both 25 and 90 °C acid reactions (see Section 4.1.2.).

We analyzed NBS-19 and two internal carbonate standards (UU-Carrara and 102-GC-AZ01) at regular intervals to monitor system stability and precision, with the following results (reported on the 'carbon dioxide equilibrium scale'): NBS-19 ($n = 23$) $\Delta_{47} = 0.414 \pm 0.018$‰ (mean $\pm 1\sigma$ standard deviation); UU-Carrara ($n = 93$) $\Delta_{47} = 0.403 \pm 0.015$‰; 102-GC-AZ01 ($n = 102$) $\Delta_{47} = 0.710 \pm 0.015$. The $\delta^{13}C$ and $\delta^{18}O$ values of the samples were normalized to concurrent analyses of NBS-19 ($\delta^{13}C = 1.95$‰ PDB, $\delta^{18}O = -2.20$‰ PDB) or an in-house Carrara marble standard calibrated to NBS-19. Statistical treatment of corrected isotopic data (e.g., comparing $\Delta_{47}$ means) was done using Kaleidagraph 4 (Synergy Software) and JMP 9 (SAS Institute Inc.). The Electronic Annex reports all isotopic data for samples, carbonate standards, and equilibrium gases, as well as information on the models, the slopes, and intercepts of equilibrium gas lines and ETFs. Thus the Electronic Annex contains all of the data necessary to recalculate $\Delta_{47}$ values and reconstruct the calibration. We present all data from all of the analytical sessions that we attempted for modern mollusks and brachiopods, including data that were judged to be poor analyses and subsequently were excluded from the final dataset.

## 3. RESULTS

The isotopic compositions ($\delta^{13}C$, $\delta^{18}O$, and $\Delta_{47}$) of the mollusk and brachiopod shells are presented in Table 1 and the mean $\Delta_{47}$ value for each shell is plotted against its assigned growth temperature in Fig. 3a. A salient feature of this calibration data is the difference in $\Delta_{47}$, at growth temperatures below ~25 °C, relative to the previous biogenic calibrations. Note that these previous calibrations have been converted to the 'carbon dioxide equilibrium scale' using the equation given in Table 4 of Dennis et al. (2011) (Fig. 3a). Bivalve mollusks from the Barents Sea have the highest $\Delta_{47}$ values, ranging from 0.788‰ to 0.745‰, and sub-sampled shell from the 27.5 °C interval of the *C. ermineus* shell from the Gulf of Mexico has the lowest $\Delta_{47}$ value of 0.656‰ (Table 1, Fig. 3). The six brachiopod $\Delta_{47}$ values plot within the range of mollusk values. Additionally, there is no clear difference in $\Delta_{47}$ between aragonitic mollusks and calcitic mollusks or brachiopods, despite the theoretical prediction of ~0.02‰ enrichment in $\Delta_{47}$ of aragonite relative to calcite in this temperature range (Schauble et al., 2006; Guo et al., 2009). The absence of aragonite–calcite fractionation is consistent with Caltech datasets for calcitic and aragonitic biogenic carbonates (e.g., Tripati et al., 2010; Thiagarajan et al., 2011), which fall on a single line that agrees well with the inorganic calcite calibration line of Ghosh et al. (2006). A least squares linear regression of the mollusk and brachiopod $\Delta_{47}$ data versus the inverse squared growth temperatures results in a calibration line ($r^2 = 0.84$):

$$\Delta_{47} = 0.0327 \times 10^6/T^2 + 0.3286 \quad (3)$$

that converges with the Ghosh et al. (2006) calibration at 31.1 °C. The statistical details of Eq. (3) are presented in Table 2. The theoretical calibration for calcite (Schauble et al., 2006) is within the error of Eq. (3) over the temperature range of the shell data. Note that this calibration is adapted to the carbon dioxide equilibrium scale via conversion of the mineral-$CO_2$ $\Delta_{47}$ 'acid' fractionation reported by Guo et al. (2009) (=0.232‰) to the carbon dioxide equilibrium scale (=0.268‰; Dennis et al., 2011, Table 4). The slope and intercept of Eq. (3) are also similar to the re-calculated Dennis and Schrag (2010) calibration within the reported errors of each regression (Dennis et al., 2011).

For comparison with previous and contemporary data cast on the 'Ghosh' scale (e.g., Ghosh et al., 2006; Huntington et al., 2009), we also report a least squares regression of the mollusk and brachiopod inverse squared growth temperatures and clumped isotope data reported in the 'older' reference frame:

$$\Delta_{47} = 0.0318 \times 10^6/T^2 + 0.2737 \quad (4)$$

It should be noted that isotopic data from the *M. edulis* shells were excluded from this calibration. During the short interval in the January–May, 2010 analytical session when these shells were analyzed (Electronic Annex) the $\Delta_{47}$ value of the carbonate standard NBS-19 was offset by $0.031 \pm 0.005$‰ (mean $\pm$ standard error of the mean) from the accepted value, which was several times greater than the offsets for other working standards run during this analytical session. This offset persisted despite our efforts to correct for temporal variability in carbonate standard $\Delta_{47}$ residuals during this analytical session, thus precluding the use of the *M. edulis* data in the $\Delta_{47}$–temperature calibration. We note, however, that these *M. edulis* $\Delta_{47}$ values, when plotted against their assigned growth temperatures, appear to agree with the trend of the mollusk and brachiopod data in Fig. 3a.

We also evaluated the ability of paired carbonate $\delta^{18}O$ and $\Delta_{47}$ analyses to predict the $\delta^{18}O$ of water in which each shell grew (Fig. 3b). This is done by converting the $\Delta_{47}$ value to an apparent temperature using Eq. (3), and then calculating the temperature dependent oxygen isotope fractionation factor between carbonate and water using

the equations of Kim and O'Neil (1997) or Kim et al. (2007) for calcite or aragonite, respectively. The standard error of the calculated $\delta^{18}O_{water}$ was determined by the propagation of error from the $\Delta_{47}$-derived temperature and measured shell $\delta^{18}O$ through the equilibrium oxygen isotope thermometry equations. In general, these comparisons revealed that seawater compositions are predicted within about 0.5‰ of measured/modeled $\delta^{18}O_{water}$, although larger deviations are not uncommon (Fig. 3b). For some localities we relied on modeled $\delta^{18}O_{water}$ values (LeGrande and Schmidt, 2006) and apparent oxygen isotope disequilibrium could be caused, in part, by error in these estimates (Table 1).

In Fig. 3a, it is apparent that a range of $\Delta_{47}$ values for mollusk and brachiopod shells are observed for a given growth temperature. This is demonstrated most clearly where there is a high density of data, for example at the Polar site B-12 in the Barents Sea where 15 shells spanning six bivalve mollusk species were analyzed. The $\Delta_{47}$ values at B-12 ranged from 0.753‰ for *C. ciliatum* to 0.784‰ for *C. islandica*, within which there appear to be real differences between individuals and perhaps between species (Table 1). One way to evaluate the 'spread' of data around the linear regression (Eq. (3)) is to evaluate if it could be created by the analytical error of $\Delta_{47}$ measurements alone. Fig. 4 plots distribution of all mollusk and brachiopod $\Delta_{47}$ measurements (i.e., not 'grouped' by means of replicate analyses), normalized by the linear regression (Eq. 3), along with a Gaussian probability density function that has a mean equal to zero and a standard deviation equivalent to long-term, repeat analyses of our in-house Carrara marble standard (=0.015‰). This comparison shows that the standard deviation of all measurements of mollusks and brachiopods (=0.018‰) is slightly greater than the measurement error of a homogeneous carbonate standard. The standard deviation for only the Arctic shells from site B-12 ($n = 46$) is 0.016‰, only slightly greater than the measurement error for our internal standards. It is conceivable that this poorer precision is an artifact of sample heterogeneity and errors in our estimates of the growth temperatures. However, the data are also consistent with a small degree of 'vital effect' disequilibrium, or simply reduced precision for analyses of natural biogenic carbonates containing complex organic matrices, relative to the precision obtained for very pure laboratory standards.

## 4. DISCUSSION

The clumped isotope calibration in this study was generated by analyzing mollusks and brachiopods across the virtual totality of ambient temperatures that they inhabit (−1.0 to 29.5 °C), as well as a number of different habitats. In the following discussion we seek explanations for why the calibration slopes of our study and Dennis and Schrag (2010) differ from those of Ghosh et al. (2006), Ghosh et al. (2007), Came et al. (2007), Tripati et al. (2010), and Thiagarajan et al. (2011). Section 4.1. explores methodological explanations and Section 4.2. explores 'biological' explanations relating to possible differences in isotopic fractionation during biomineralization in different taxonomic groups.

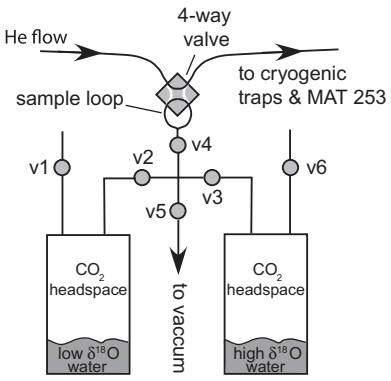


Fig. 2. Carbon dioxide–water equilibration device used to generate 'reference' $CO_2$ gases in equilibrium with two isotopically different waters at controlled temperatures. Both reservoirs are submerged in a thermostatic water bath that maintains a constant temperature of 30 (or 27) ± 1 °C. The 4-port, 2-way valve is shown in the 'standby' position where the valve and lines to the automated extraction device (described in Section 2) are purged with a purified He carrier gas. During standby the sample loop is open to a rough pump via valves 4 and 5. During sample analysis, the sample loop is filled with $CO_2$ gas from either reservoir by closing valve 5 and opening valve 4, and then opening either valve 2 or 3. Valve 4 is then closed, and switching of the 4-port valve introduces the $CO_2$ in the sample loop to the automated preparation device. The $CO_2$ immediately passes through a −78 °C trap, and is treated in exactly the same manner as sample $CO_2$ (i.e., from carbonate) except that it bypasses the phosphoric acid/autosampler volume.

### 4.1. Methodological explanations

#### *4.1.1. Intercalibration between different laboratories*

A simple explanation for the observed differences in calibrations is that different laboratories are poorly intercalibrated. Prior to 2011, published carbonate clumped isotope data were reported on a 'heated gas' reference frame, which used $CO_2$ heated to 1000 °C to create a stochastic distribution of $^{13}C$–$^{18}O$ bonds (Ghosh et al., 2006; Huntington et al., 2009). These gases were analyzed along with samples and used to construct a reference line to which measured $\Delta_{47}$ values could be compared. A problem with this method was that the $\Delta_{47}$ value of the heated gases was defined as 0‰, effectively assuming that the reference line represented a completely disordered state after spending a sufficient amount of time (~2 h) at a high temperature (~1000 °C). However, theoretical predictions of $\Delta_{47}$ by Wang et al. (2004) suggested that $CO_2$ heated to 1000 °C has an equilibrium $\Delta_{47}$ value of 0.027‰. The heated gas reference frame also relied on an empirically-derived correction factor to account for $CO_2$ fragmentation and/or recombination reactions in the ionization source which may 'scramble' or reorder the $^{13}C$–$^{18}O$ bonds in the analyte gas (Huntington et al., 2009). Use of this 'scale compression' or 'stretching' factor requires the assumption that different tanks of Oztech reference $CO_2$ used in different laboratories have the same $\Delta_{47}$ value, or alternatively it requires calibration of a reference gas to gases previously analyzed relative to the original Oztech reference gas at the California Institute of Technology (Caltech) used in the Ghosh et al. (2006) calibration study. NBS-19 served as

the only widely available reference material for evaluating the soundness of the correction scheme through time, and indeed most laboratories reported broadly similar $\Delta_{47}$ values for this material. However, its $\Delta_{47}$ value, ~0.35‰, is far outside of the range of low temperature calibrations (0.55–0.78‰ on the 'Ghosh' scale).

Dennis et al. (2011) readdressed the issue of interlaboratory standardization of clumped isotope measurements by establishing an empirical reference frame that tied measured $\Delta_{47}$ values of $CO_2$ to theoretical predictions of $\Delta_{47}$ of $CO_2$ at given equilibration temperatures. They showed that by using this revised reference frame, which we refer to as the carbon dioxide equilibrium scale (CDES), interlaboratory agreement on a set of natural carbonates was at least 0.017‰ (1$\sigma$ standard deviation), and as good as 0.008‰ (1$\sigma$ standard deviation). These differences are too small to account for the greatest difference (~0.08‰) observed between $\Delta_{47}$–temperature calibrations at the coldest mollusk and brachiopod growth temperatures.

We directly tested for interlaboratory agreement by distributing an aliquot of aragonitic shell from specimen Ha-3 (*H. arctica*, site B-12, western Barents Sea) for analysis at Yale University and Caltech. Ha-3 was chosen for this comparison because the $\Delta_{47}$ values of shells from the Arctic site B-12 are the most different from the $\Delta_{47}$ value predicted by the Ghosh et al. (2006) calibration. Of the 15 individual shells analyzed from B-12, Ha-3 had abundant material and a $\Delta_{47}$ value (0.776‰) that was close to the group mean of 0.770‰. The raw clumped isotope data ($\delta_{47}$, $\Delta_{47}$) from Yale and Caltech were corrected using a static heated gas line and compared to our measured value for Ha-3 on the 'Ghosh' scale (Table 3). Unfortunately, these analyses were made before all laboratories were routinely reporting $\Delta_{47}$ data on the carbon dioxide equilibrium scale, thus precluding the use of the revised reference frame in these comparisons. The reported $\Delta_{47}$ value from Yale is 0.021‰ higher than our measurement and the Caltech value is 0.008‰ higher, but neither was high enough to account for the difference between the Caltech calibrations and the JHU + Harvard calibrations (Table 3, Fig. 5). However, these differences do highlight the importance of reporting $\Delta_{47}$ values on the CDES reference frame, as it was designed to empirically account for source fragmentation or recombination reactions during carbonate sample, standard, and equilibrium reference gas analysis. Given these results and those of the interlaboratory calibration presented by Dennis et al. (2011), it seems that the different slopes of the Caltech and JHU + Harvard calibrations cannot be explained by poor interlaboratory calibration. However, these intercalibration exercises are imperfect for addressing this question, because the methodologies used at Caltech for these exercises are not the same as those used for the Caltech calibration studies. The former utilized the newer 90 °C acid reaction, packed GC column, online technique, whereas the latter utilized the original 25 °C acid reaction, capillary GC column, offline method. However, the methodology used at Yale for the interlaboratory calibration exercises are similar to the original methods used for the Caltech calibrations.

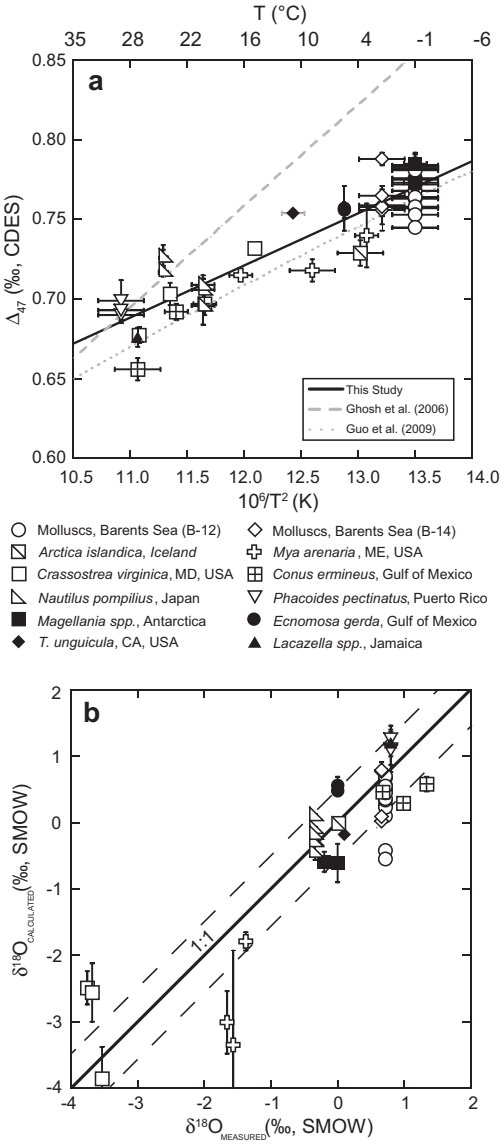


Fig. 3. (a) All $\Delta_{47}$ measurements of mollusk and brachiopod shells versus their growth temperatures. The solid black line is a linear regression through the mollusk and brachiopod data and the dashed and dotted grey lines are the empirical (Ghosh et al., 2006) and theoretical (Guo et al., 2009) calibrations for calcite, respectively. Clumped isotope data are reported on the carbon dioxide equilibrium scale or 'CDES' (Dennis et al., 2011), whereas data in Fig. 1 are reported on the 'Ghosh' scale (Ghosh et al., 2006). Error bars on $\Delta_{47}$ represent the standard error of the mean from multiple analyses of a single shell, and error bars on $10^6/T^2$ are the temperature ranges from Table 1. (b) Calculated $\delta^{18}O$ of seawater (using the measured carbonate $\delta^{18}O$ and the apparent clumped isotope temperatures from mollusks and brachiopods) versus the measured $\delta^{18}O$ of seawater at each collection location. For aragonitic mollusks the inorganic aragonite equilibrium oxygen isotope fractionation equation of Kim et al. (2007) was used to calculate seawater $\delta^{18}O$. For calcitic brachiopods and mollusks the inorganic calcite oxygen isotope equilibrium equation of Kim and O'Neil (1997) was used instead. The dashed lines are ± 0.5‰ deviation from the 1:1 line and are shown only for reference.

*4.1.2. Acid temperature*

The Caltech calibrations (Ghosh et al., 2006, 2007; Came et al., 2007; Tripati et al., 2010; Thiagarajan et al., 2011) utilized 25 °C phosphoric acid reactions, whereas this study and Dennis and Schrag (2010) utilized 90 °C reactions. Thus it is critical that the difference in acid fractionation factor between 90 and 25 °C is accurately known, where the acid fractionation factor $\Delta^* = \Delta_{47,CO_2} - \Delta_{63,CaCO_3}$ (Guo et al., 2009). $\Delta_{47,CO_2}$ is the composition of $CO_2$ generated by phosphoric acid reaction of carbonate, and $\Delta_{63,CaCO_3}$ is the composition of the carbonate mineral. Passey et al. (2010) estimated the difference in $\Delta^*$ between 25 and 90 °C reactions, $\Delta^*_{25-90}$, by analyzing homogenous carbonates using both a 90 °C, packed GC column, online extraction line, as well as by 25 °C, capillary GC column, offline extractions. All analyses were conducted at Caltech, but using two different mass spectrometers. The observed value for $\Delta^*_{25-90}$, 0.081‰, is not a pure estimate of the acid temperature effect, because the approach convolved acid temperature, extraction method, and different mass spectrometers. Likewise, the interlaboratory calibrations of Dennis et al. (2011) and those reported in Section 4.2. convolve several methodological aspects, only one of which is acid temperature.

Therefore we undertook an experiment to measure $\Delta^*_{25-90}$ using a single extraction line and mass spectrometer. We studied three mollusk shells, two from the Arctic collection site B-12 and one from Puerto Rico (Table 4). The 25 °C reactions were conducted in McCrea-type vessels for ~12 h, with the vessels immersed in a constant temperature water bath. The vessels were then attached to our automatic gas preparation line and the $CO_2$ was extracted in the same way as our regular 90 °C analyses. The same materials were also analyzed using 90 °C reactions. The mean $\Delta^*_{25-90}$ was $0.076 \pm 0.007$‰ ($1\sigma$ standard deviation; on the 'Ghosh' scale), similar to the 0.081‰ offset determined by Passey et al. (2010). The mean $\Delta^*_{25-90}$ for the carbon dioxide equilibrium scale is $0.092 \pm 0.012$‰ ($1\sigma$ standard deviation). The differences among these values are not large enough to explain discrepancies between calibrations (Fig. 3a).

In summary, we find no convincing explanation for why the carbonate clumped isotope calibration for mollusks and brachiopods should be different than the existing inorganic and biogenic calibration data (e.g., Ghosh et al., 2006). Our interlaboratory $\Delta_{47}$ comparisons of shell Ha-3 add to previous comparisons, which have now been completed on a suite of natural carbonates (Fig. 5). These data should be viewed as the most realistic comparisons of interlaboratory reproducibility because they make no effort to evaluate any single aspect of making a carbonate clumped isotope measurement. If $\Delta_{47}$ calibration measurements made at Johns Hopkins were dramatically different from measurements currently being made at Caltech, Yale, or Harvard, it should be apparent in a comparison such as Fig. 5.

### 4.2. Biological explanations

It is conceivable that mollusks and brachiopods have a unique response of $\Delta_{47}$ to temperature, possibly owing to differences in biomineralization mechanisms. In the biological systems relevant to this discussion, carbonate formation occurs in semi-isolated volumes which have varying degrees of connectivity with the ambient environment (Weiner and Dove, 2003). The chemical composition and mineral precipitation kinetics within these volumes is therefore a function of some combination of (a) the biological influence on the chemistry of the precipitating fluid (e.g., ionic transport or metabolic activity) and (b) the ambient seawater chemistry. While the design of our study does not allow us to evaluate the isotopic interplay between biology and seawater directly, we can discuss isotopic effects associated with the chemical and physical conditions of marine carbonate biomineralization.

Table 2
Linear regression of mollusk and brachiopod shell $\Delta_{47}$ values versus their growth temperatures.

| Linear regression | $\Delta_{47} = 0.0327 \times 10^6/T^2 + 0.3286$ |
|---|---|
| Shells used | 45 |
| $R^2$ | 0.84 |
| RMSE[a] | 0.15 |
| Intercept standard error (‰) | 0.0278 |
| Intercept $t$ ratio[b] | 11.83 |
| Slope standard error (‰/$10^6/T^2$) | 0.0022 |
| Slope $t$ ratio[b] | 14.83 |

[a] The square root of the mean squared error.
[b] The ratio of the linear regression parameters to their respective standard errors. For example, a value greater than 2 is significant at the 0.05 significance interval.

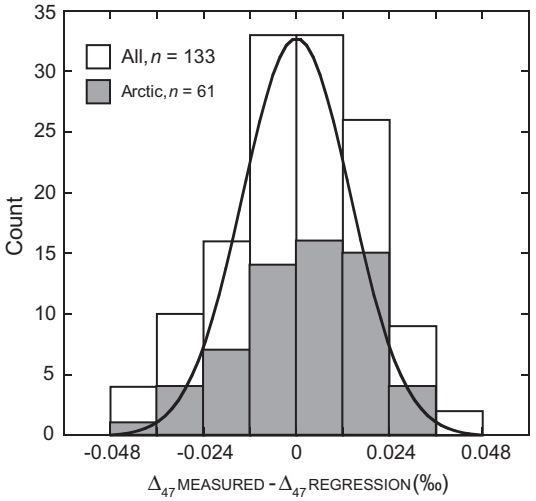


Fig. 4. Distribution of all $\Delta_{47}$ measurements plotted as the difference between the measured $\Delta_{47}$ and the growth temperature-equivalent $\Delta_{47}$ predicted by Eq. (3). The distribution of $\Delta_{47}$ values for only the Arctic bivalves (sites B-12 and B-14) is shown in grey. The black line represents a Gaussian distribution of $\Delta_{47}$ data around a mean of 0‰ with a standard deviation of 0.015‰, which is the long-term standard deviation of our in-house Carrara marble standard. The $\Delta_{47}$ data used to create the 'All' and 'Arctic' histograms are from individual analysis of mollusk and brachiopod shell material. This differs from Fig. 2 which presents the $\Delta_{47}$ data as the mean of replicate analyses on a single specimen.

#### 4.2.1. Isotopic mixing

The non-linear effect on $\Delta_{47}$ resulting from mixing carbonates with different bulk isotopic compositions has been predicted from theory and demonstrated by experiment (Eiler and Schauble, 2004). In our study, this effect is a concern when two or more regions of a shell with different $\delta^{13}C$ and $\delta^{18}O$ may be combined for analysis or during biomineralization when the shell itself may be formed from two isotopically distinct reservoirs of dissolved inorganic carbon (DIC). In either case, mixing will cause the resultant $\Delta_{47}$ to be greater than the weighted sum of the end member $\Delta_{47}$ values (Eiler and Schauble, 2004). Mollusk and brachiopod shell $\delta^{13}C$ and $\delta^{18}O$ vary in accordance with seasonal environmental conditions such as productivity, temperature, and the isotopic composition of water (e.g., Mii and Grossman, 1994; Buening and Spero, 1996; Goodwin et al., 2003; Gentry et al., 2008; McConnaughey and Gillikin, 2008; Wanamaker et al., 2011; Beirne et al., 2012). The clumped isotopic composition of shells used in this calibration that were sub-sampled indiscriminately across all growth bands could therefore incorporate a pronounced mixing effect. To evaluate this effect we consider a 50/50 mixing of end-member $\delta^{13}C$ and $\delta^{18}O$ values for shell grown during a hypothetical mid-latitude summer ($\delta^{13}C = 0‰$, $\delta^{18}O = -2‰$) and winter ($\delta^{13}C = 1.5‰$, $\delta^{18}O = 1.5‰$). The result is a $\Delta_{47}$ mixing effect of 0.0014‰. If the Ghosh et al. (2006) calibration represents the $\Delta_{47}$–temperature relationship that all biocarbonates (including mollusks and brachiopods) should have, then mixing isotopically different parts of a shell would cause a shift in the wrong direction (positive) with a magnitude that would be too small to explain the difference between calibrations.

#### 4.2.2. Amorphous calcium carbonate

An alternative to the mixing effect caused by combination of shell regions with different isotopic compositions is a different kind of mixing effect due to the presence of multiple phases of calcium carbonate. When material for this calibration was sub-sampled from mollusk shells containing both aragonite and calcite, we carefully selected one over the other (e.g., calcite from *M. edulis*). Recent analysis of mollusk shells, however, has demonstrated that amorphous calcium carbonate (ACC) may be a component of juvenile and adult mollusk shell as a precursory phase (Weiss et al., 2002; Jacob et al., 2011) that is unresolvable by traditional methods for mineralogical identification (e.g., X-ray diffraction). The physical and thermochemical properties of ACC have been described (Radha et al., 2010), but the stable isotopic composition of ACC relative to non-amorphous phases of calcium carbonate (calcite or aragonite) is unknown. Therefore, it is impossible to speculate on the effect of incorporating residual molluskan (or brachiopod) ACC in our carbonate clumped isotope measurements. In an effort to reduce any putative contribution of ACC to our analyte $CO_2$, we pretreated two shells in a pH-buffered calcium acetic acid solution (1 M, pH = 4.6) at 4 °C for 24 h. This pretreatment was envisioned to preferentially dissolve ACC over aragonite. We observed no effect of this pretreatment on the $\Delta_{47}$ value of the shells (Table 5), implying that either no appreciable ACC was present initially, pretreatment was ineffective at removing ACC, or ACC did not significantly affect the isotopic composition of untreated shell. Regardless, the paucity of isotopic data from amorphous phases of calcium carbonate highlights an important avenue for further research as it has been suggested to be an important transitional phase during carbonate biomineralization in mollusks, echinoderms, and arthropods (Adaddi et al., 2003).

#### 4.2.3. Diffusion

Extensional molluskan shell growth occurs directly along the ventral margin from the extrapallial fluid (EPF), which is enclosed in a cavity between the inner shell surface and the mantle. The ionic and organic composition of the EPF distinguishes it from seawater and suggests active biological control over the conditions of shell precipitation (Crenshaw, 1972). It has been hypothesized that at least some of the calcium ions and DIC in the EPF is supplied by the hemolymph to the outermost mantle cells (Lowenstam and Weiner, 1989), which is supported by recent studies on the carbon isotope composition of ambient DIC and coeval shell (e.g., Beirne et al., 2012). Thus, isotope effects from the diffusion of dissolved $CO_2$ across cellular membranes or through body fluids should be considered in light of the observed discrepancies between clumped isotope calibrations.

Isotopic fractionation due to diffusion of $CO_2$ through the phospholipid bilayer is often invoked in 'vital effect' models for carbonate biomineralization (Erez, 2003; Cohen and McConnaughey, 2003). As Thiagarajan et al. (2011) point out in their discussion of clumped isotope compositions of corals, Knudsen diffusion, in which gas passes through a pore with a diameter that is less than the mean free path of the diffusing molecule, predicts that the diffused gas will be depleted in heavy isotopes relative to the residual gas according to the equation:

$$R_{\text{diffused}}/R_{\text{residual}} = \sqrt{m_1/m_2} \tag{5}$$

where $R_{\text{diffused}}$ and $R_{\text{residual}}$ are the isotope ratios of the diffused and residual gases and $m_1$ and $m_2$ are masses of isotopologues 1 and 2. For an aliquot of $CO_2$ gas that has undergone Knudsen diffusion the diffused gas will be lower in $\delta^{13}C$ and $\delta^{18}O$ by 11.3‰ and 22.5‰, respectively, but 0.5‰ higher in $\Delta_{47}$ (Eiler and Schauble, 2004). A nonstochastic value of $\Delta_{47}$ in the diffused gas results from the non-linear dependence of $\Delta_{47}$ on the bulk isotopic composition of the gas (Eiler and Schauble, 2004; Thiagarajan et al., 2011).

The isotopic fractionation associated with diffusion of $CO_2$ through a different gas (e.g., air) can be calculated using the following equation:

$$R_{\text{diffused}}/R_{\text{residual}} = \sqrt{((M_2 + M_{\text{air}})/(M_2 M_{\text{air}}))} \times ((M_1 M_{\text{air}})/(M_1 + M_{\text{air}})) \tag{6}$$

where, again, $R_{\text{diffused}}$ and $R_{\text{residual}}$ are the isotope ratios of the diffused and residual gases, $M_1$ and $M_2$ are masses of isotopologues 1 and 2, and $M_{\text{air}}$ is the average atomic mass of air. The gas-phase diffusion of $CO_2$ through air results in decreases for $\delta^{13}C$ and $\delta^{18}O$ in the diffused gas by 4.4‰ and

Table 3
Interlaboratory $\Delta_{47}$ comparison using shell Ha-3 (Site B-12, Barents Sea).

| Laboratory | $n$ | $\delta^{13}C_{carb}$ (‰, PDB) | $\delta^{18}O_{carb}$ (‰, PDB) | $\Delta_{47}$ (‰, Ghosh) | $\lvert q\rvert$[a] | $P$-value[b] | Null ($\alpha = 0.1$) |
|---|---|---|---|---|---|---|---|
| Johns Hopkins University | 3 | 0.41 (±0.03) | 5.05 (±0.04) | 0.719 (±0.005) | – | – | – |
| Yale University | 4 | 0.68 (±0.02) | 4.93 (±0.03) | 0.741 (±0.015) | 1.55 | 0.60 | Cannot reject |
| California Institute of Technology | 3 | 0.47 (±0.03) | 5.03 (±0.07) | 0.727 (±0.013) | 0.66 | 0.89 | Cannot reject |

*Notes:* All ± values are standard error of the mean ($=1\sigma/\sqrt{n}$), where $1\sigma$ is the standard deviation of the $n$ analyses. Yale $\Delta_{47}$ data were corrected using a source fragmentation/recombination scaling factor of −0.87‰. JHU and Caltech data were corrected using a −0.8453‰ scaling factor (Huntington et al. 2009). If −0.8453‰ is used in the Yale correction then the Yale $\Delta_{47}$ becomes 0.720‰.

[a] Analysis of variance (ANOVA) Tukey HSD post hoc test $q$ statistic. A large value (approximately an order of magnitude greater than the reported values) indicates statistical significance.

[b] The $P$-value associated with the $q$ statistic. If the value is below a threshold ($\alpha = 0.1$) the conclusion would be that there is a difference between groups.

8.7‰, respectively, and a positive fractionation of 0.3‰ for $\Delta_{47}$. However, Thiagarajan et al. (2011) point out that while illustrative of the magnitude and direction of isotope effects associated with pin-hole and gaseous diffusion, the fractionations determined by Eqs. (5) and (6) are clearly not applicable to aqueous systems at relatively low temperatures where the behavior of fluids deviates strongly from that of ideal gases. O'Leary (1984) experimentally determined a −0.7‰ carbon isotope fractionation associated with diffusion of $CO_2$ through water, which was less than what is predicted by solving Eq. (6) using the atomic mass of water as "$M_{air}$". Thiagarajan et al. (2011) extrapolated this result using a power law relationship between the magnitude of fractionation and the ratio of isotopologue masses to determine the isotope fractionation associated with $CO_2$ diffusion through water for $\delta^{18}O$, −1.6‰, and $\Delta_{47}$, 0.036‰.

Based on this information, we examine two different scenarios.

(i) The carbonates studied in the Caltech calibrations have greater isotopic contributions from diffused DIC, leading to elevated $\Delta_{47}$ values, and this contribution increases with decreasing temperature, leading to a steeper $\Delta_{47}$–$T$ slope. If this scenario is correct, then it is fortuitous that the methods used to precipitate calcite in the laboratory (Ghosh et al., 2006) contributed similar amounts of 'diffused' DIC to the site of mineralization as reaches the sites of mineralization in natural corals, foraminifera, and coccoliths (Tripati et al., 2010; Thiagarajan et al., 2011). Furthermore, if this scenario were correct, we would expect to see corresponding depletions in $\delta^{13}C$ and $\delta^{18}O$. While there is certainly evidence of this in the coral dataset (Thiagarajan et al., 2011, Fig. 6), there is no clear evidence of such in the inorganic data (Ghosh et al., 2006) or the foramifera and coccolith data (Tripati et al., 2010). We therefore regard this scenario as an unsatisfactory explanation for the differences between the Caltech calibrations and the JHU or Harvard calibrations.

(ii) Mollusks and brachiopods, and the inorganic carbonates precipitated by Dennis and Schrag (2010), incorporate DIC from reservoirs out of which DIC has diffused. Thus these carbonates incorporate residual DIC with low $\Delta_{47}$ that is left over after part of the DIC has diffused from the mineralization environment. If this scenario is correct, then we should observe corresponding enrichments in $\delta^{13}C$ and $\delta^{18}O$ in mollusk and brachiopod carbonate. Fig. 3b shows that, at least for $\delta^{18}O$, there is no consistent enrichment over expected values. Additionally, this scenario is unsatisfactory because DIC should be diffusing into, not out of, the extrapallial fluid environment during mineralization, because mineralization itself consumes DIC.

In summary, diffusive mechanisms do not explain all of the observed data, and cannot be the sole reason for the observed differences in calibration.

#### 4.2.4. pH and dissolved inorganic carbon speciation

It has been demonstrated that the equilibrium oxygen isotope fractionation between the sum of the DIC species and water decreases with increasing pH (Usdowski et al., 1991). This effect arises because the equilibrium oxygen isotope fractionations between DIC and water decrease in the order $CO_2$–$H_2O$; $HCO_3^-$–$H_2O$; and $CO_3^{2-}$–$H_2O$. Therefore, because the relative concentrations of DIC species change strongly as a function of pH, so too will the oxygen isotope difference between total DIC and water (see Zeebe and Wolf-Gladrow, 2001 for review). Beck et al. (2005) determined equilibrium oxygen isotope fractionation factors between $CO_2$ and $H_2O$, $HCO_3^-$ and $H_2O$, and $CO_3^{2-}$ and $H_2O$, and showed that $\delta^{18}O$ of total DIC can vary with pH by as much as 17‰ at a single temperature. The pH isotope effect is an important consideration because there is a large range of pH values observed in body fluids of carbonate mineralizing marine organisms. Among these taxa mollusks are unique in that their extrapallial fluid (EPF) has a pH value that is slightly lower than seawater and 0.5–1.5 pH units less than the precipitating fluids of foraminifera, surface corals, and fishes (pH $\geqslant$ 8; Crenshaw, 1972).

Currently, only theoretical predictions of the equilibrium clumped isotope compositions of different inorganic carbon species are available (Guo, 2009; Guo et al., 2012). At 300 K, $HCO_3^-$ is predicted to be 0.018‰ enriched in $^{13}C$–$^{18}O$ bonds relative to $CO_3^{2-}$, but may be as large as 0.04‰ (Guo et al., 2012). As an end-member scenario, if mollusk shells derive carbonate only from $HCO_3^-$, and corals and foraminifera only from $CO_3^{2-}$, then mollusks may be

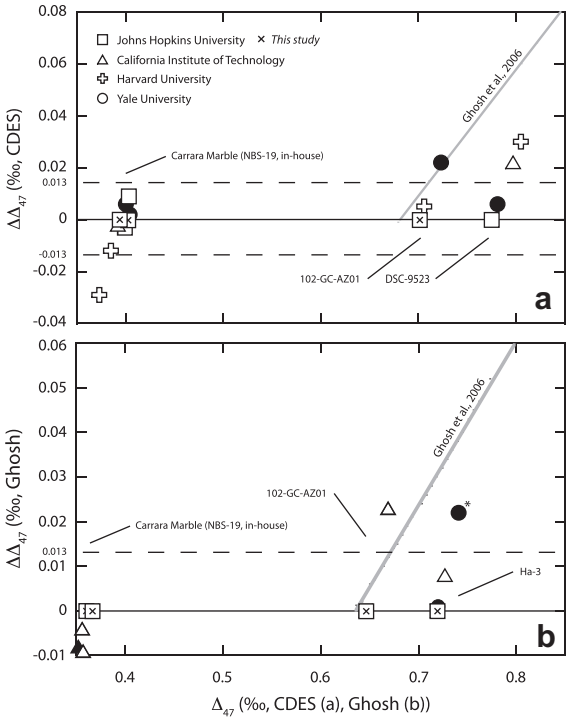


Fig. 5. A compilation of interlaboratory clumped isotope comparisons. ΔΔ47 is the clumped isotope difference between measurements at Johns Hopkins University and other laboratories ($\Delta\Delta_{47} = \Delta_{47,\mathrm{JHU}} - \Delta_{47,\mathrm{other}}$). Open symbols represent data generated using a 90 °C phosphoric acid reaction, whereas the solid symbols represent those done at 25 °C. The dashed lines in (a) and (b) are the long-term precision ($\pm 1\sigma$ standard deviation) of $\Delta_{47}$ measurements made on an in-house Carrara marble at JHU. The asterisk in (b) identifies the Yale University measurement of Ha-3 corrected using their preferred source fragmentation/recombination scaling factor of −0.87‰, instead of the −0.8453‰ used at JHU and Caltech (Table 3; Huntington et al., 2009). Data for the Carrara marbles, 102-GC-AZ01, and DSC-9253 on the CDES scale are from Dennis et al. (2011) and this study. Data for the Carrara marbles, 102-GC-AZ01, and Ha-3 on the 'Ghosh' scale are from Passey et al. (2010), Csank et al. (2011), and this study (Table 3). In (a) the grey line labeled (Ghosh et al., 2006) represents the difference between the Ghosh et al. (2006) calibration and the mollusk and brachiopod calibration (Eq. (3)). In (b) the grey line labeled (Ghosh et al., 2006) represents the difference between the Ghosh et al. (2006) calibration the theoretical calibration for calcite from Guo et al. (2009).

~0.04‰ higher in $\Delta_{47}$ than corals and foraminifera. This offset is of insufficient magnitude, and more importantly of the wrong sign, to explain the difference in the $\Delta_{47}$ versus temperature relationships between these taxa. However, experimental observations of the effects of pH and DIC speciation on $\Delta_{47}$ have not yet been described, and given the importance of DIC speciation to the isotopic composition of carbonate and the nearly 2 unit range of pH values observed in biomineralizing organisms, it will be important to characterize these effects.

#### 4.2.5. DIC disequilibrium

For the temperature range 0–50 °C, $CO_2$ has significantly higher $\Delta_{47}$ values than does carbonate at the same temperature (Fig. 7). The equilibrium clumped isotopic compositions of $CO_2$ and $CO_3^{2-}$ over a range of temperatures define the end-member values of a domain that may be useful for evaluating the differences between clumped isotope calibrations. We consider a hypothetical system where $CO_2$, which has a higher equilibrium $\Delta_{47}$ than $CO_3^{2-}$ at a given temperature, is incorporated into the biomineral through the DIC system without fully re-equilibrating to $\Delta_{47}$ compositions of $CO_3^{2-}$. Thus the mineral 'inherits' some of the high $\Delta_{47}$ of the original $CO_2$. Because of longer timescales of equilibration at lower temperatures, the $^{13}C$–$^{18}O$ inheritance from $CO_2$ would be enhanced at low temperatures, leading to an artificially steep $\Delta_{47}$ versus $T$ slope. Several scenarios may be envisioned where these kinetics would be relevant, including the incorporation of diffused $CO_2$ into fast growing biogenic carbonate (e.g., Adkins et al., 2003) or rapid biochemical pH change to induce mineralization from invaginated seawater (e.g., foraminifera; Bentov et al., 2009).

Additionally, a complicated interplay of chemical and isotope exchange kinetics of DIC ultimately determines the isotopic composition of biogenic carbonates. The rate constants of the carbonate system are not well understood relative to the equilibrium constants, but they may be used to compare with equivalent isotope exchange reaction rates (Zeebe and Wolf-Gladrow, 2001). For example, the forward reaction rate constant for the hydrolysis reaction:

$$HCO_3^- + OH^- \rightarrow CO_3^{2-} + H_2O$$

is $k = 6 \times 10^9\ \mathrm{kg\ mol^{-1}\ s^{-1}}$ at 20 °C, which for ~2.5 mmol $kg^{-1}$ of $HCO_3^-$ is practically instantaneous (Eigen, 1964). In contrast, the oxygen isotope exchange reaction between bicarbonate and water:

$$HC^{16}O_3^- + H_2^{18}O \rightarrow HC^{18}O^{16}O_2^- + H_2^{16}O$$

can take hours to tens of hours (depending on the ambient temperature and pH) to reach equilibrium, implying comparatively slow reaction kinetics (Beck et al., 2005). Thus in a closed system with a rapid precipitation rate it is possible to rapidly dissociate bicarbonate into carbonate without establishing isotopic equilibrium prior to precipitation in the mineral phase. This kinetic effect has been invoked to explain carbonate ion effects on the oxygen isotope compositions of synthetic and natural carbonates (Usdowski et al., 1991; Spero et al., 1997; Adkins et al., 2003).

Dissolved $CO_2$ plays an important role in coral and foraminifera mineralization, and is involved in Kim and O'Neil-type laboratory precipitation experiments similar to those used by Ghosh et al. (2006). Thus it is conceivable that the clumped isotope composition of $CO_2$ could be imprinted on synthetic calcium carbonates. In scleractinian corals it has been hypothesized that the enzyme $Ca^{2+}$ ATPase drives calcification by pumping calcium ions across cellular membranes, causing aragonite supersaturation in the precipitating fluid (Adkins et al., 2003; Cohen and McConnaughey, 2003). The currency of extracellular ion exchange by $Ca^{2+}$ ATPase is the proton, whose removal from the precipitating fluid causes the pH to increase, thereby dissociating $HCO_3^-$ to $CO_3^{2-}$. Carbonate precipitation results in a net $CO_2$ diffusion across the cellular membrane to

Table 4
$\Delta_{47}$ Acid correction factors based on acid reactions at 90 and 25 °C using mollusk shells.

| Sample ID | Sample species/ type | *n* | $\Delta_{47}$ (‰, Ghosh) autoline, 90 °C | $\Delta_{47}$ (‰, CDES) autoline, 90 °C | $\Delta_{47}$ (‰, Ghosh) offline, 25 °C[a] | $\Delta_{47}$ (‰, CDES) offline, 25 °C | Acid correction (‰, Ghosh) | Acid correction (‰, CDES) |
|---|---|---|---|---|---|---|---|---|
| Ha-3 (B-12) | *Hiatella arctica* | 3 | 0.638 | 0.684 | 0.714 | 0.783 | 0.076 | 0.099 |
| Ac-1 (B-12) | *Astarte crenata* | 3 | 0.630 | 0.689 | 0.699 | 0.767 | 0.069 | 0.078 |
| Pp-3 | *Phacoides pectinatus* | 3 | 0.548 | 0.601 | 0.630 | 0.700 | 0.082 | 0.099 |
| | | | | | | Mollusk average | 0.076 | 0.092 |
| | | | | | | 1$\sigma$ SD | 0.007 | 0.012 |
| | | | | | | Passey et al. (2010)[b] | 0.081 | – |
| | | | | | | Guo et al. (2009)[c] | 0.069 | – |

[a] 'Offline' reactions done *in vacuo* for ~12 h at 25 °C using $\rho = 1.91$ phosphoric acid. Evolved $CO_2$ was cleaned by cryogenic trapping and gas chromatography using the same sample purification as the automated preparation device acid reactions at 90 °C. See Section 2.2.
[b] Empirically derived.
[c] Theoretically derived.

the calcification site. Carbon dioxide diffusion could also be caused by $CO_2$ removal by photosynthesis (this would not be the case for non-symbiotic corals) or $CO_2$ hydration reactions that fail to keep pace with $CaCO_3$ precipitation. The presence of another enzyme, carbonic anhydrase, may accelerate the $CO_2$ hydration reaction when the growth of the biogenic carbonate is limited by carbonate ion supply (Cohen and McConnaughey, 2003), but we feel that this would only strengthen our hypothetical scenario where $CO_2$ carries at least part of its equilibrium clumped isotopic composition to the mineral phase.

Marine foraminifera also manipulate pH to control the calcite or aragonite saturation state of their precipitating fluids, which are small-volumes of endocytosed seawater (Erez, 2003). Like corals, a pH change in the precipitating vacuole of a foraminifera causes the enclosed DIC (i.e., ambient seawater) to shift to mostly $CO_3^{2-}$, and if the internal pH is higher than the external pH this causes $CO_2$ diffusion into the endocytosing vacuole. It is possible that metabolic $CO_2$ also diffuses into these vacuoles. Regardless, for both corals and foraminifera, it seems plausible that some of the C–O bonds in carbonate could be inherited from $CO_2$ without equilibration as $CO_3^{2-}$. The superficial similarities between the modern coral and foraminifera clumped isotope data are linked by a similar mechanism for inducing calcium carbonate supersaturation in their calcifying fluids (Cohen and McConnaughey, 2003; Erez, 2003).

To evaluate this '$CO_2$ inheritance' hypothesis, we may again turn to carbon and oxygen isotopes. For low temperature conditions (0–30 °C), the $\delta^{13}C$ of dissolved $CO_2$ is approximately 10‰ lower than that of carbonate, and $\delta^{18}O$ is approximately 20‰ higher than carbonate (Mook, 1986; Zhang et al., 1995; Beck et al., 2005). It is impossible for a DIC species to reach carbon and oxygen isotope equilibrium without also reaching clumped isotopologue equilibrium, so any disequilibrium isotope effect seen in $\Delta_{47}$ should also be reflected in $\delta^{13}C$ and $\delta^{18}O$. As an end-member scenario, we assume that no isotopic fractionation is associated with the initial conversion of $CO_2$ to $CO_3^{2-}$:

$$CO_2(aq) + H_2O \leftrightarrow H_2CO_3 \rightarrow HCO_3^- + H^+ \rightarrow CO_3^{2-} + 2H^+$$

Thus the initial (unequilibrated) $CO_3^{2-}$ will have a $\Delta_{47}$ value ~0.3‰ higher than equilibrated $CO_3^{2-}$, $\delta^{13}C$ −10‰ lower, and $\delta^{18}O$ 20‰ higher. The offset between the Caltech calibrations and the theoretical calibrations at 0 °C is about 0.08‰. Under this scenario about 25% of the carbonate ions in the final carbonate mineral would have to inherit their $\Delta_{47}$ value from unequilibrated $CO_2$. The corresponding fractionations in $\delta^{13}C$ and $\delta^{18}O$ should be about −2.5‰, and +5‰, respectively. Such large fractionations are not observed. This implies that either the overall scenario of 'inherited' $CO_2$ clumping is incorrect, or that the assumption of zero isotope fractionation during the initial synthesis of $CO_3^{2-}$ from $CO_2 + H_2O$ is grossly in error. Both of these possibilities can presumably be addressed by additional theoretical and experimental work.

## 5. SUMMARY

This paper presents the results of carbonate clumped isotope analyses performed on modern marine mollusk and brachiopod shells, which spanned virtually the entire range of growth temperatures found in modern oceans. Regressed against the inverse squared shell growth temperature, these data form a calibration line, $\Delta_{47} = 0.0327 \times 10^6/T^2 + 0.3286$, whose temperature sensitivity (slope) is approximately half that of similar calibrations done on biogenic carbonates and inorganic laboratory precipitates (Fig. 3a; Ghosh et al., 2006, 2007; Tripati et al., 2010; Thiagarajan et al., 2011). This study

Table 5
Stable isotope data from sample pretreatment experiments using pH-buffered acetic acid.

| Sample ID | Species | *n* | Pretreatment[a] | $\delta^{13}C_{carb}$ (‰, PDB) | $\delta^{18}O_{carb}$ (‰, PDB) | $\Delta_{47}$ (‰, Ghosh) | $\Delta_{47}$ (‰, CDES) | *P*-value[b] |
|---|---|---|---|---|---|---|---|---|
| Ha-4 (B-12) | *Hiatella arctica* | 2 | 0.1 M pH-buffered acetic acid | 1.03 (±0.03) | 4.98 (±0.02) | 0.680 | 0.751 (±0.002) | 0.33 |
| Ha-4 (B-12) | *Hiatella arctica* | 2 | Deionized water (control) | 0.99 (±0.08) | 4.98 (±0.01) | 0.672 | 0.741 (±0.006) | – |
| Pp-2 | *Phacoides pectinatus* | 2 | 0.1 M pH-buffered acetic acid | 0.82 (±0.02) | −0.70 (±0.01) | 0.620 | 0.688 (±0.028) | 0.80 |
| Pp-2 | *Phacoides pectinatus* | 3 | None | 0.77 (±0.01) | −0.70 (±0.02) | 0.632 | 0.699 (±0.013) | – |

*Note:* All ± values are standard deviation (1$\sigma$).
[a] The pretreatment was for 12 h at room temperature after sonicating twice for 5 min each.
[b] *P*-values from a Wilcoxon–Mann–Whitney rank sum test. Values greater than $\alpha = 0.1$ indicate no significant differences between treatments and control values.

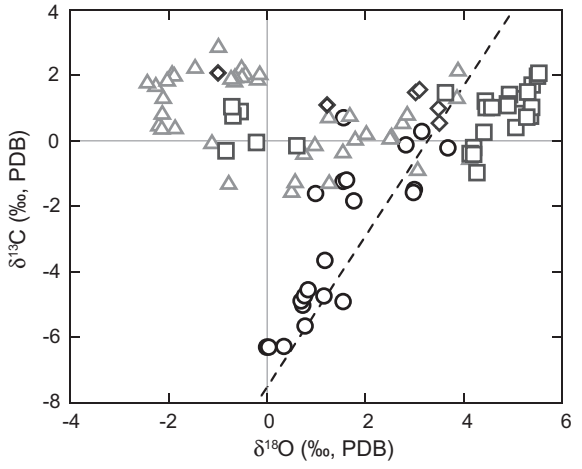


Fig. 6. Carbon isotope versus oxygen isotope crossplot for mollusk, brachiopod, coral, and foraminifera samples used in empirical carbonate clumped isotope calibrations. Mollusk (dark gray squares) and brachiopod (dark gray diamonds) shells from this study; deep-sea corals from Thiagarajan et al. (2011; black circles), and foraminifera from Tripati et al. (2010; gray triangles). The dashed line is the average linear regression of deep-sea coral stable isotope compositions in Adkins et al. (2003): $\delta^{13}C = 2.3 \times \delta^{18}O - 7.5$. Agreement between the Thiagarajan et al. (2011) data and the average regression confirms the presence of an Adkins et al. (2003)-type vital effect in these samples. There is no clear relationship between $\delta^{13}C$ and $\delta^{18}O$ for mollusks, brachiopods, and foraminifera.

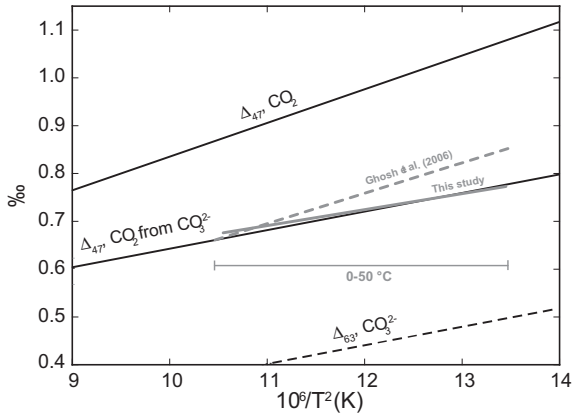


Fig. 7. Theoretical predictions of the temperature dependence of $\Delta_{47}$ of $CO_2$ (solid black line; Wang et al., 2004), $\Delta_{47}$ of $CO_2$ liberated from calcite by phosphoric acid digestion at 25 °C (solid black line; Guo et al., 2009), and of $\Delta_{63}$ for $CO_3^{2-}$ (dashed black line; Schauble et al., 2006). These curves illustrate the ~0.3‰ difference between $CO_2$ and $CO_2$ generated from calcite at earth surface temperatures (~0 to 50 °C). The empirical $\Delta_{47}$–temperature calibration of Ghosh et al. (2006) and Eq. (3) from this study are shown as grey dashed and solid lines, respectively.

is unique in that it is the only clumped isotope calibration to date that uses newer analytical methods (i.e., 'hot' phosphoric acid reaction, polymer-packed gas chromatography column, and automated sample preparation), and is fully referenced to the 'carbon dioxide equilibrium scale' reference frame (Dennis et al., 2011). Potential methodological causes for discrepancies between calibrations, including poor interlaboratory calibration and error in the acid temperature correction, were found to be relatively minor compared to the magnitude of calibration disagreement. Biological explanations for the different temperature sensitivity of the mollusk and brachiopod calibration were also addressed. The isotopic effects associated with mechanical mixing and diffusion, as they pertain to biomineralization, were predicted to have small effects on the clumped isotope composition of shell. We addressed some of the physical and chemical aspects of shells and the chemical conditions of their formation, such as the potential incorporation of amorphous calcium carbonate into the analyzed material and the isotopic consequences of taxonomic differences in precipitating fluid pH. These effects are predicted to not affect shell clumped isotope compositions, although more data are needed to fully understand the effects of pH and ACC on the isotopic composition of biogenic carbonate. Finally, we used a simple kinetic model for clumped isotopic disequilibrium in biogenic carbonates to evaluate the possibility of $CO_2$, whose clumped isotope composition is ~0.3‰ higher than $CO_3^{2-}$ at a given temperature, 'imprinting' its composition on carbonate ions incorporated into rapidly growing carbonate. This is an attractive explanation for the differences between calibrations because of the superficial similarities of coral and foraminifera biomineralization, but is untenable given the bulk isotopic compositions (e.g., $\delta^{13}C$, $\delta^{18}O$) of these carbonates.

Despite differences in calibration, the clumped isotope thermometer remains an alluring technique for carbonate paleothermometry and reconstruction of the oxygen isotopic composition of precipitating fluids. Clumped isotope thermometry is an emerging method – only a handful of laboratories currently make the measurement, the field has just recently been introduced to a normalization scheme that can be reliably reproduced in different laboratories (Dennis et al., 2011), and experimental and empirical calibrations continue to emerge. There are many aspects of carbonate isotopologue systematics that remain to be described, such as equilibrium fractionations between coexisting species of DIC, kinetic fractionations during transformations of DIC species, and temperature and pH-dependent rates of exchange among coexisting isotopologues. This kind of knowledge, combined with improved analytical techniques and standardized methods of data normalization, will continue to improve our ability to interpret clumped isotope compositions of natural carbonates in terms of temperature and other parameters.

## ACKNOWLEDGEMENTS

This work has benefited from the generosity of several individuals who without which we would not have had the opportunity to analyze such a wide range of specimens: C. Del Castillo collected shells from the La Parguera region of Puerto Rico, T. Moritaki provided deceased nautilus from the Toba Aquarium, J. Scourse provided the *A. islandica* shell from Iceland, and D. Merritt provided access to the aquaculture facilities at the Horn Point Laboratory. We would also like to thank H. Affek and P. Douglas at Yale University and R. Eagle and J. Eiler at Caltech for their participation in the inter-laboratory comparison exercise (Table 3). This manuscript has benefitted from numerous discussions with J. Ferry, D. Sverjensky, W. Guo, N. Levin, T. Haine, M. Suarez, and S. Li. We are also grateful to two anonymous reviewers, whose comments further improved the clarity of this manuscript. This research was supported by the Department of Earth and Planetary Sciences at Johns Hopkins University, and collection of the Barents Sea mollusks was supported by the Norwegian Research Council, under the International Polar Year program.

## APPENDIX A. SUPPLEMENTARY DATA

Supplementary data associated with this article can be found, in the online version, at http://dx.doi.org/10.1016/j.gca.2012.12.020.

## REFERENCES

Adaddi L., Raz S. and Weiner S. (2003) Taking advantage of disorder: amorphous calcium carbonate and its roles in biomineralization. *Adv. Mater.* **15**, 959–970.

Adkins J. F., Boyle E. A., Curry W. B. and Lutringer A. (2003) Stable isotopes in deep-sea corals and a new mechanism for "vital effects". *Geochim. Cosmochim. Acta* **67**, 1129–1143.

Beck W. C., Grossman E. L. and Morse J. W. (2005) Experimental studies of oxygen isotope fractionation in the carbonic acid system at 15° 25° and 40°C. *Geochim. Cosmochim. Acta* **69**, 3493–3503.

Beirne E. C., Wanamaker, Jr., A. D. and Feindel S. C. (2012) Experimental validation of environmental controls on the $\delta^{13}C$ of *Arctica islandica* (ocean quahog) shell carbonate. *Geochim. Cosmochim. Acta* **84**, 395–409.

Bentov S., Brownlee C. and Erez J. (2009) The role of seawater endocytosis in the biomineralization process in calcareous foraminifera. *Proc. Natl. Acad. Sci. U.S.A.* **106**, 21500–21504.

Buening N. and Spero H. J. (1996) Oxygen- and carbon-isotope analyses of the articulate brachiopod *Laqueus californianus*: a recorder of environmental changes in the subeuphotic zone. *Mar. Biol.* **127**, 105–114.

Came R. E., Eiler J. M., Veizer J., Azmy K., Brand U. and Weidman C. R. (2007) Coupling of surface temperatures and atmospheric $CO_2$ concentrations during the Palaeozoic era. *Nature* **449**, 198–201.

Carroll M. L., Ambrose, Jr., W. G., Levin B. S., Ryan S. K., Ratner A. R., Henkes G. A. and Greenacre M. J. (2011) Climatic regulation of *Clinocardium ciliatum* (bivalvia) growth in the northwestern Barents Sea. *Palaeogeogr. Palaeoclimatol. Palaeoecol.* **302**, 10–20.

Cohen A. L. and McConnaughey T. A. (2003) Geochemical perspectives on coral mineralization. In *Biomineralization* (eds. P. M. Dove, J. J. De Yoreo and S. Weiner). Reviews in Mineralogy and Geochemistry, Washington, pp. 151–182.

Crenshaw M. A. (1972) The inorganic composition of molluscan extrapallial fluid. *Biol. Bull.* **143**, 506–512.

Csank A. Z., Tripati A. K., Patterson W. P., Eagle R. A., Rybczynski N., Ballantyne A. P. and Eiler J. (2011) Estimates of Arctic land surface temperatures during the early Pliocene from two novel proxies. *Earth Planet. Sci. Lett.* **304**, 291–299.

Dennis K. J. and Schrag D. P. (2010) Clumped isotope thermometry of carbonatites as an indicator of diagenetic alteration. *Geochim. Cosmochim. Acta* **74**, 4110–4122.

Dennis K. J., Affek H. P., Passey B. H., Schrag D. P. and Eiler J. M. (2011) Defining an absolute reference frame for 'clumped' isotope studies of $CO_2$. *Geochim. Cosmochim. Acta* **75**, 7117–7131.

Eigen M. (1964) Proton transfer, acid–base catalysis, and enzymatic hydrolysis. *Angew. Chem. Int. Ed. Engl.* **3**, 1–19.

Eiler J. M. and Schauble E. A. (2004) $^{18}O^{13}C^{16}O$ in Earth's atmosphere. *Geochim. Cosmochim. Acta* **68**, 4767–4777.

Epstein S., Buchsbaum R., Lowenstam H. A. and Urey H. C. (1953) Revised carbonate-water isotopic temperature scale. *Geol. Soc. Am. Bull.* **64**, 1315–1325.

Erez J. (2003) The source of ions for biomineralization in foraminifera and their implications for paleoceanographic proxies. In *Biomineralization* (eds. P. M. Dove, J. J. De Yoreo and S. Weiner). Reviews in Mineralogy and Geochemistry, Washington, pp. 115–144.

Finnegan S., Bergmann K., Eiler J. M., Jones D. S., Fike D. A., Eisenman I., Hughes N. C., Tripati A. K. and Fischer W. W. (2011) The magnitude and duration of late Ordovician-Early Silurian glaciation. *Science* **331**, 903–906.

Gentry D. K., Sosdian S., Grossman E. L., Rosenthal Y., Hicks D. and Lear C. H. (2008) Stable isotope and Sr/Ca profiles from the marine gastropod *Conus ermineus*: testing a multiproxy approach for inferring paleotemperature and paleosalinity. *Palaios* **23**, 195–209.

Ghosh P., Adkins J., Affek H., Balta B., Guo W., Schauble E. A., Schrag D. P. and Eiler J. M. (2006) $^{13}C$–$^{18}O$ bond in carbonate minerals: a new kind of paleothermometer. *Geochim. Cosmochim. Acta* **70**, 1439–1456.

Ghosh P., Eiler J., Campana S. E. and Feeney R. F. (2007) Calibration of the carbonate 'clumped isotope' paleothermometer for otoliths. *Geochim. Cosmochim. Acta* **71**, 2736–2744.

Goodwin D. H., Schöne B. R. and Dettman D. L. (2003) Resolution and fidelity of oxygen isotopes as paleotemperature proxies in bivalve mollusk shells: models and observations. *Palaios* **18**, 110–125.

Guo W. (2009) Carbonate clumped isotope thermometry: application to carbonaceous chondrites and effects of kinetic isotope fractionation. Ph. D. thesis, California Institute of Technology.

Guo W., Mosenfelder J. L., Goddard, III, W. A. and Eiler J. M. (2009) Isotopic fractionations associated with phosphoric acid digestion of carbonate minerals: insight from first-principles theoretical modeling and clumped isotope measurements. *Geochim. Cosmochim. Acta* **73**, 7203–7225.

Guo W., Kim S.-T., Yuan J., Farquhar J. and Passey B. H. (2012) $^{13}C$–$^{18}O$ bonds in dissolved inorganic carbon: toward a better understanding of clumped isotope thermometer in biogenic carbonates. *Mineral. Mag.* **76**, 1791.

Grossman E. L. and Ku T.-L. (1986) Oxygen and carbon isotope fractionation in biogenic aragonite: temperature effects. *Chem. Geol.* **59**, 59–74.

Harris C. L., Plueddemann A. J. and Gawarkiewicz G. G. (1998) Water mass distribution and polar front structure in the western Barents Sea. *J. Geophys. Res.* **103**, 2905–2917.

Huntington K. W., Eiler J. M., Affek H. P., Guo W., Bonifacie M., Yeung L. Y., Thiagarajan N., Passey B. H., Tripati A., Daëron M. and Came R. (2009) Methods and limitations of 'clumped' $CO_2$ isotope ($\Delta_{47}$) analysis by gas-source isotope ratio mass spectrometry. *J. Mass Spectrom.* **44**, 1318–1329.

Jacob D. E., Wirth R., Soldati A. L., Wehrmeister U. and Schreiber A. (2011) Amorphous calcium carbonate in the shells of adult Unionoida. *J. Struct. Biol.* **173**, 241–249.

Jackson J. B. C. and Winston J. E. (1982) Ecology of cryptic coral reef communities: 1. Distribution and abundance of major groups of encrusting organisms. *J. Exp. Mar. Biol. Ecol.* **57**, 135–147.

Johannessen O. M. and Foster L. A. (1978) A note on the topographically controlled oceanic Polar Front in the Barents Sea. *J. Geophys. Res.* **83**, 4567–4571.

Keating-Bitonti C. R., Ivany L. C., Affek H. P., Douglas P. and Samson S. D. (2011) Warm, not super-hot, temperatures in the early Eocene subtropics. *Geology* **39**, 771–774.

Kim S.-T. and O'Neil J. R. (1997) Equilibrium and nonequilibrium oxygen isotope effects in synthetic carbonates. *Geochim. Cosmochim. Acta* **61**, 3461–3475.

Kim S.-T., O'Neil J. R., Hillaire-Marcel C. and Mucci A. (2007) Oxygen isotope fractionation between synthetic aragonite and water: influence of temperature and $Mg^{2+}$ concentration. *Geochim. Cosmochim. Acta* **71**, 4704–4715.

Knudsen K. L., Eiriksson J., Jansen J., Jiang H., Rytter F. and Gudmundsdottir E. R. (2004) Paleoceanographic changes off North Iceland through the last 1200 years: foraminifera, stable isotope, diatoms, and ice-rafted debris. *Quatern. Sci. Rev.* **23**, 2231–2246.

LeGrande A. N. and Schmidt G. A. (2006) Global gridded data set of the oxygen isotopic composition in seawater. *Geophys. Res. Lett.* **33**, L12604, 5pp..

Lowenstam H. A. and Weiner S. (1989) *On Biomineralization*. Oxford University Press, New York, pp. 99–103.

McConnaughey T. A. and Gillikin D. P. (2008) Carbon isotopes in mollusk shell carbonates. *Geo-Mar. Lett.* **28**, 287–299.

Mii H.-S. and Grossman E. L. (1994) Late Pennsylvanian seasonality reflected in the $^{18}O$ and elemental composition of a brachiopod shell. *Geology* **22**, 661–664.

Mook W. G. (1986) $^{13}C$ in atmospheric $CO_2$. *Neth. J. Sea Res.* **20**, 211–223.

O'Leary M. H. (1984) Measurement of the isotope fractionation associated with diffusion of carbon dioxide in aqueous solution. *J. Phys. Chem.* **88**, 823–825.

Passey B. H., Levin N. E., Cerling T. E., Brown F. H. and Eiler J. M. (2010) High-temperature environments of human evolution in East Africa based on bond ordering in paleosol carbonates. *Proc. Natl. Acad. Sci. U.S.A.* **107**, 11245–11249.

Radha A. V., Forbes T. Z., Killian C. E., Gilbert P. U. P. A. and Navrotsky A. (2010) Transformation and crystallization energetic of synthetic and biogenic amorphous calcium carbonate. *Proc. Natl. Acad. Sci. U.S.A.* **107**, 16438–16443.

Rooker J. R. and Dennis G. D. (1991) Diel, lunar and seasonal changes in a mangrove fish assemblage off southwestern Puerto Rico. *Bull. Mar. Sci.* **49**, 684–698.

Schauble E. A., Ghosh P. and Eiler J. M. (2006) Preferential formation of $^{13}C$–$^{18}O$ bonds in carbonate minerals, estimated using first-principles lattice dynamics. *Geochim. Cosmochim. Acta* **70**, 2510–2529.

Schrag D. P. and DePaolo D. J. (1993) Determination of $\delta^{18}O$ of seawater in the deep ocean during the last glacial maximum. *Paleoceanography* **8**, 1–6.

Skagseth Ø., Furevik T., Ingvaldsen R., Loeng H., Mork K. A., Orvik K. A. and Ozhigin V. (2008) Volume and heat transports to the Arctic Ocean via the Norwegian and Barents Seas. In *Arctic–Subarctic Ocean Fluxes: Defining the Role of the Northern Sea in Climate*. Springer, The Netherlands, pp. 45–64.

Spero H. J., Bijma J., Lea D. W. and Bemis B. E. (1997) Effect of seawater carbonate concentration on foraminiferal carbon and oxygen isotopes. *Nature* **390**, 497–500.

Thiagarajan N., Adkins J. and Eiler J. (2011) Carbonate clumped isotope thermometry of deep-sea coral and implications for vital effects. *Geochim. Cosmochim. Acta* **75**, 4416–4425.

Tripati A. K., Eagle R. A., Thiagarajan N., Gagnon A. C., Bauch H., Halloran P. R. and Eiler J. M. (2010) $^{13}C$–$^{18}O$ isotope signatures and 'clumped isotope' thermometry in foraminifera and coccoliths. *Geochim. Cosmochim. Acta* **74**, 5697–5717.

Usdowski E., Michaelis J., Bottcher M. E. and Hoefs J. (1991) Factors for the oxygen isotope equilibrium fractionation between aqueous and gaseous $CO_2$, carbonic-acid, bicarbonate, carbonate, and water (19 °C). *Z. Phys. Chem. Neue Folge* **170**, 237–249.

Wanamaker, Jr., A. D., Heinemeier J., Scourse J. D., Richardson C. A., Butler P. G., Eiriksson J. and Knudsen K. L. (2008) Very long-lived mollusks confirm 17th century AD tephra-based radiocarbon reservoir ages for North Icelandic Shelf waters. *Radiocarbon* **50**, 399–412.

Wanamaker, Jr., A. D., Hetzinger S. and Halfar J. (2011) Reconstructing mid- to high-latitude marine climate and ocean variability using bivalves, coralline algae, and marine sediment cores from the Northern Hemisphere. *Palaeogeogr. Palaeoclimatol. Palaeoecol.* **302**, 1–9.

Wanamaker, Jr., A. D., Kreutz K. J., Borns, Jr., H. W., Introne D. S., Feindel S., Funder S., Rawson P. D. and Barber B. J. (2007) Experimental determination of salinity, temperature, growth and metabolic effects on shell isotope chemistry of *Mytilus edulis* collected from Maine and Greenland. *Paleoceanography* **22**, PA2217, 12 pp..

Wang Z., Schauble E. A. and Eiler J. M. (2004) Equilibrium thermodynamics of multiply substituted isotopologues of molecular gases. *Geochim. Cosmochim. Acta* **68**, 4779–4797.

Weiner S. and Dove P. M. (2003) An overview of biomineralization processes and the problem of the vital Effect. In *Biomineralization* (eds. P. M. Dove, J. J. De Yoreo and S. Weiner). Reviews in Mineralogy and Geochemistry, Washington, pp. 1–29.

Weiss I. M., Tuross N., Addadi L. and Weiner S. (2002) Mollusc larval shell formation: amorphous calcium carbonate is a precursor phase for aragonite. *J. Exp. Zool.* **293**, 478–491.

Winter A., Appeldoorn R. S., Bruckner A., Williams, Jr., E. H. and Goenaga C. (1998) Sea surface temperature and coral reef bleaching off La Parguera, Puerto Rico (northeastern Caribbean Sea). *Coral Reefs* **17**, 377–382.

Zaarur S., Olack G. and Affek H. P. (2011) Paleo-environmental implication of clumped isotopes in land snail shells. *Geochim. Cosmochim. Acta* **75**, 6859–6869.

Zeebe R. E. and Wolf-Gladrow D. (2001) $CO_2$ in seawater: equilibrium, kinetics, isotopes. *Elsevier Oceanography Series* **65**, 4–10.

Zhang J., Quay P. D. and Wilbur D. O. (1995) Carbon isotope fractionation during gas-water exchange and dissolution of $CO_2$. *Geochim. Cosmochim. Acta* **59**, 107–114.

*Associate editor:* Robert H. Byrne